



CERN-EP-2018-095
9 May 2018

**Measurements of low- p_T electrons from semileptonic heavy-flavour
hadron decays at mid-rapidity in pp and Pb–Pb collisions
at $\sqrt{s_{NN}} = 2.76$ TeV**

ALICE Collaboration*

Abstract

Transverse-momentum (p_T) differential yields of electrons from semileptonic heavy-flavour hadron decays have been measured in the most central (0–10%) and in semi-central (20–40%) Pb–Pb collisions at $\sqrt{s_{NN}} = 2.76$ TeV. The corresponding production cross section in pp collisions has been measured at the same energy with substantially reduced systematic uncertainties with respect to previously published results. The modification of the yield in Pb–Pb collisions with respect to the expectation from an incoherent superposition of nucleon-nucleon collisions is quantified at mid-rapidity ($|y| < 0.8$) in the p_T interval 0.5–3 GeV/ c via the nuclear modification factor, R_{AA} . This paper extends the p_T reach of the R_{AA} measurement towards significantly lower values with respect to a previous publication. In Pb–Pb collisions the p_T -differential measurements of yields at low p_T are essential to investigate the scaling of heavy-flavour production with the number of binary nucleon-nucleon collisions. Heavy-quark hadronization, a collective expansion and even initial-state effects, such as the nuclear modification of the Parton Distribution Function, are also expected to have a significant effect on the measured distribution.

© 2018 CERN for the benefit of the ALICE Collaboration.

Reproduction of this article or parts of it is allowed as specified in the CC-BY-4.0 license.

*See Appendix A for the list of collaboration members

1 Introduction

In ultra-relativistic heavy-ion collisions at the Relativistic Heavy-Ion Collider (RHIC) and at the Large Hadron Collider (LHC), strongly-interacting matter characterized by high energy density and temperature is produced [1–6]. Under these conditions, the formation of a deconfined state of quarks and gluons, called Quark-Gluon Plasma (QGP), is predicted by Quantum ChromoDynamic (QCD) calculations on the lattice [7–11]. The production of heavy quarks, i.e. charm (c) and beauty (b), takes place via initial partonic scattering processes with large momentum transfer (hard scattering) on a timescale of $\hbar/(2m_{c,b}c^2)$, where m is the mass of the quark. This timescale (e.g. ≈ 0.08 fm/c for charm) is smaller than the QGP thermalization time (≈ 0.6 – 1 fm/c [12]). Additional thermal production as well as annihilation rates of charm and beauty quarks in the strongly interacting medium are expected to be small in Pb–Pb collisions even at LHC energies [13–15]. Consequently, charm and beauty quarks are ideal probes to investigate the properties of the QGP, since they experience the full evolution of the strongly interacting medium produced in high-energy heavy-ion collisions.

In order to exploit the sensitivity of heavy-flavour observables to medium effects a precise reference where such effects are not expected is needed and it is provided by pp collisions. In pp collisions, heavy-quark production can be described theoretically via perturbative QCD calculations over the full quark momentum range, while such a description does not hold for gluon and light-quark production [13]. Therefore, measurements of heavy-flavour production cross sections in pp collisions are used to test perturbative QCD calculations and provide the necessary experimental reference for heavy-ion collisions.

The modification of the p_T -differential yield in heavy-ion collisions with respect to pp collisions at the same centre-of-mass energy is quantified by the nuclear modification factor R_{AA} , defined as:

$$R_{AA}(p_T, y) = \frac{1}{\langle T_{AA} \rangle} \cdot \frac{d^2 N_{AA}/dp_T dy}{d^2 \sigma_{pp}/dp_T dy} \quad (1)$$

where $d^2 N_{AA}/dp_T dy$ is the yield measured in heavy-ion collisions in a given p_T and y interval, and $d^2 \sigma_{pp}/dp_T dy$ is the corresponding production cross section in pp collisions. The average nuclear overlap function, $\langle T_{AA} \rangle$, is given by the ratio of the average number of binary nucleon-nucleon collisions in a centrality class and the inelastic nucleon-nucleon cross section, and it is determined via Glauber model calculations [16, 17]. In the absence of medium effects, R_{AA} is expected to be unity for hard probes such as charm and beauty production.

For momenta larger than the masses of charm and beauty quarks, the dominant medium effect is the partonic energy loss via radiative [18, 19] and collisional processes [20–22] when heavy quarks propagate through the QGP. These processes are expected to cause a shift of the partonic momentum distribution towards lower momenta and, therefore, to lead to a suppression of the yield of heavy-flavour hadrons and their decay products at high p_T ($\gtrsim 2$ GeV/c) and, consequently, to $R_{AA} < 1$. In the absence of further processes that modify the total charm and/or beauty production cross section or the fragmentation/hadronization of heavy quarks, R_{AA} is expected to increase again towards low p_T to compensate the suppression at high p_T and, therefore, conserve the binary collision scaling. At RHIC, such a rise was observed by the PHENIX and STAR experiments for leptons from semileptonic heavy-flavour hadron decays in Au-Au and Cu-Cu collisions at $\sqrt{s_{NN}} = 200$ GeV [23–26]. The STAR Collaboration also measured the R_{AA} of D^0 mesons in Au-Au collisions for $p_T < 8$ GeV/c [27].

The interaction of charm and, to a lesser extent, beauty quarks of low transverse momentum with the medium may lead to the participation of heavy quarks in the collective expansion of the hot and dense system [28, 29] and, eventually, to a partial or complete thermalization of heavy quarks in the system [30]. Moreover, while in pp collisions charm and beauty quarks hadronize via fragmentation, in heavy-ion collisions a competing hadronization mechanism through the coalescence with other quarks from the

medium could become relevant and modify the phase-space distribution of heavy-flavour hadrons up to transverse momenta of a few GeV/c [31–33]. Finally, initial-state effects due the presence of a heavy nucleus in the collision system can play a role. At low Bjorken- x (below 10^{-2}) the parton densities in nucleons bounded in nuclei are reduced with respect to those in free nucleons. This so-called "shadowing" leads to a reduction of heavy-flavour production, becoming more pronounced with decreasing p_T [34]. In addition, at lower collision energies, momentum (k_T) broadening leads to an enhancement of R_{AA} at intermediate p_T , the so-called Cronin effect [35].

At the LHC, open heavy-flavour production was measured in Pb–Pb collisions via exclusive hadron decays of prompt D and B mesons and via leptons from heavy-flavour hadron decays [36–43]. At high p_T ($\gtrsim 3$ GeV/c), a substantial suppression with respect to the scaled reference cross section from pp collisions is observed with R_{AA} values similar to those measured at RHIC. At lower p_T , the R_{AA} of prompt D mesons stays below unity down to transverse momenta as low as 1 GeV/c, in contrast to corresponding measurements at RHIC where R_{AA} reaches a maximum value of ≈ 1.5 at $p_T \approx 1\text{--}2$ GeV/c. The different patterns observed at the LHC and at RHIC could be due to differences in the initial momentum distributions of heavy quarks, the magnitude of parton energy loss in the medium, the impact of collective expansion, the relevance of coalescence as a hadronization mechanism, and the role of initial-state effects [43].

At the LHC, initial-state effects and their impact on the nuclear modification factor are investigated in proton-lead (p–Pb) collisions. The nuclear modification factor R_{pPb} was measured at mid-rapidity for prompt D and B mesons and for electrons from semileptonic heavy-flavour hadron decays [38, 44–46]. The R_{pPb} of electron from heavy-flavour hadron decay was observed to be consistent with unity within uncertainties over the whole p_T range of the measurements, as expected from binary-collision scaling of heavy-flavour production.

This paper reports on measurements of electrons from semileptonic heavy-flavour hadron decays at mid-rapidity ($|\eta| < 0.8$) in pp collisions at $\sqrt{s} = 2.76$ TeV and in Pb–Pb collisions in the two centrality classes 0–10% and 20–40% at $\sqrt{s_{NN}} = 2.76$ TeV. The charge averaged p_T -differential yields, cross sections and the resulting nuclear modification factors are presented. Applying a data-driven background subtraction technique [45] allowed for a reduction of the systematic uncertainties of the pp reference cross section by a factor of about 3 compared to the previously published reference [47], which is consistent within uncertainties with the current measurement.

The results presented in this paper extend the previous measurements [42] of electrons from semileptonic heavy-flavour hadron decays in Pb–Pb collisions from 3 GeV/c down to 0.5 GeV/c in p_T . They complement the measurements of muons from semileptonic heavy-flavour hadron decays at forward rapidity and of the prompt D mesons at mid-rapidity reported by the ALICE Collaboration [39, 41], as well as of muons from semileptonic heavy-flavour hadron decays at mid-rapidity reported by the ATLAS Collaboration [48]. The measured nuclear modification factor R_{AA} is compared with model calculations aiming at describing heavy-quark production and energy loss in heavy-ion collisions taking into account also initial-state effects.

2 Experimental apparatus and data sample

The ALICE apparatus, described in detail in [49, 50], consists mainly of a central barrel at mid-rapidity ($|\eta| < 0.9$) embedded in a solenoidal magnet, and a muon spectrometer at forward rapidity ($-4 < \eta < -2.5$). In the following, the subsystems which are used to perform the measurement of electrons from heavy-flavour hadron decays are described.

Charged-particle tracks are reconstructed at mid-rapidity ($|\eta| < 0.9$) with the Inner Tracking System (ITS) and the Time Projection Chamber (TPC). The ITS [51] consists of six cylindrical silicon layers

surrounding the beam vacuum pipe. The first two layers, made of Silicon Pixel Detectors (SPD) to cope with the high particle density in the proximity of the interaction point, provide an excellent position resolution of $12\ \mu\text{m}$ and $100\ \mu\text{m}$ in the $r\phi$ and the beam direction (z -coordinate of the reference system), respectively. The third and fourth layers consist of Silicon Drift Detectors (SDD), while the two outermost layers are made of Silicon Strip Detectors (SSD). The SDD and SSD layers are also used for charged-particle identification via energy loss (dE/dx) measurements.

The TPC [52] is the main tracking detector in the central barrel and provides a charged-particle momentum measurement together with excellent two-track separation and particle identification via dE/dx determination.

The Time-Of-Flight (TOF) detector [53] provides the measurement of the time-of-flight for charged particles from the interaction point up to the detector radius of 3.8 m, with an overall resolution of about 80 ps. The measured time-of-flight of electrons is well separated from that of kaons and protons up to $p_T \simeq 2.5\ \text{GeV}/c$ and $p_T \simeq 4\ \text{GeV}/c$, respectively.

The V0 detectors [54] consist of two arrays of 32 scintillator tiles covering the pseudorapidity ranges $2.8 < \eta < 5.1$ (V0A) and $-3.7 < \eta < -1.7$ (V0C), respectively, and are used for triggering and for centrality estimation. The latter is performed through a Glauber Monte Carlo (MC) fit of the signal amplitude in the two scintillator detectors [55–57]. Together with the Zero Degree Calorimeters (ZDC) [58], located on both sides of the interaction point at $z \approx \pm 114\ \text{m}$, they are used offline for event selection.

The pp results presented in this paper are based on the same minimum-bias (MB) data sample recorded at $\sqrt{s} = 2.76\ \text{TeV}$ as the previously published result [47]. The MB trigger required at least one hit in the SPD or a signal (above threshold) in either of the two V0 arrays, in temporal coincidence with a signal from the beam position monitors [50]. Pile-up events are identified and rejected using the SPD [47, 59], and they amount to about 0.7% of all events. During the pp run at 2.76 TeV, the information from the SDD was read out only for a fraction of the recorded events to maximize the data acquisition speed. For the current analysis all events have been reconstructed without the SDD information in order to obtain a homogeneous sample over the full statistics.

For the Pb–Pb analysis, the same data sample recorded at $\sqrt{s_{NN}} = 2.76\ \text{TeV}$ was used as for previous publications [28, 42]. The events were collected with a MB interaction trigger using information from the coincidence of signals between the V0A and V0C detectors. Central and semi-central Pb–Pb collisions were selected online by applying different thresholds on the V0 signal amplitudes resulting in central (0–10%) and semi-central (10–50%) trigger classes [50]. Events affected by pile-up from different bunch crossings have been rejected offline [28]. This selection removes up to 5% of the total number of events depending on the centrality of the collisions.

For both collision systems, only events with a reconstructed interaction vertex (primary vertex) within 10 cm from the nominal interaction point along the beam direction are used in order to minimize edge effects at the limit of the central barrel acceptance. The number of events analysed after applying the event selection and the corresponding luminosities for the pp and the two Pb–Pb centrality classes are listed in Table 1. The values of the average nuclear overlap function for the two Pb–Pb centrality classes are listed as well. These values and the respective uncertainties are updated with respect to the previously published high- p_T R_{AA} results [42]. More information about the update of the average nuclear overlap function values can be found in [60].

3 Data analysis

The p_T -differential yield of electrons from semileptonic heavy-flavour hadron decays is computed by measuring the inclusive electron yield and subtracting the contribution of electrons that do not originate from open heavy-flavour hadron decays. In the following, the inclusive electron identification strategy

Collision system	N_{events}	$\langle T_{AA} \rangle$ (mb $^{-1}$)
pp	38.9×10^6	–
Pb–Pb, 0–10%	15.4×10^6	23.37 ± 0.2
Pb–Pb, 20–40%	8.2×10^6	7.109 ± 0.15

Table 1: Number of events for the pp collisions and the two Pb–Pb centrality classes after applying the event selection. In the right column the average nuclear overlap function is reported for the Pb–Pb samples [60].

and the subtraction of electrons originating from background sources are described for the analysis of pp and Pb–Pb collisions.

3.1 Track selection and electron identification

Candidate electrons tracks are required to fulfil the criteria summarized in Table 2, similarly to what was done in Refs. [28, 47], in order to select good quality tracks. The rapidity range used in the analyses is restricted to $|y| < 0.8$ to exclude the edges of the detectors, where the systematic uncertainties related to particle identification increase.

Data Sample	Pb–Pb	pp
p_T range (GeV/ c)	0.5–3	0.5–3
$ y $	< 0.8	< 0.8
Number of TPC clusters	≥ 100	≥ 110
Number of TPC clusters in dE/dx calculation	≥ 90	≥ 80
Ratio of found TPC clusters over findable	> 0.6	> 0.6
$\chi^2/\text{clusters}$ of the momentum fit in the TPC	< 3.5	< 4
DCA $_{xy}$	< 2.4 cm	< 1 cm
DCA $_z$	< 3.2 cm	< 2 cm
Number of ITS hits	≥ 5	≥ 3
Number of hits in the SPD layers	2	2

Table 2: Track selection criteria used in the analyses. DCA is an abbreviation for the distance of closest approach of a track to the primary vertex.

The electron identification is mainly based on the measurement of the specific ionization energy loss in the TPC (dE/dx), similarly to the procedure followed in Refs. [28, 47]. The discriminant variable is the deviation of dE/dx from the parametrized electron Bethe-Bloch [61] expectation value, expressed in units of the dE/dx resolution, n_{σ}^{TPC} [50].

In order to reduce the hadron contamination in Pb–Pb collisions, tracks with a time-of-flight differing from the expected value for electrons (n_{σ}^{TOF}) by twice the TOF resolution or more are rejected. In pp collisions, a $|n_{\sigma}^{\text{TOF}}| \geq 3$ rejection is applied due to the smaller hadron contamination.

In Pb–Pb collisions, in addition, the dE/dx in the ITS is used to further reject hadrons. To guarantee a good Particle IDentification (PID) based on the dE/dx in the ITS, tracks are required to have at least three out of the four possible hits in the external layers of the ITS (SDD and SSD), which can provide dE/dx measurements. Table 3 summarizes the PID selection criteria for electron identification.

The remaining hadron contamination is estimated by fitting in momentum slices the TPC dE/dx distribution after the TOF (and ITS) PID selections [28, 59]. The hadron contamination is negligible at the lowest p_T and it increases with p_T , reaching about 5% at $p_T = 3$ GeV/ c in Pb–Pb collisions and about 1%

	p_T range (GeV/c)	TPC dE/dx selection	ITS dE/dx selection	TOF compatibility with e hypothesis
pp	0.5–3	$-1 < n_{\sigma}^{\text{TPC}} < 3$	–	$ n_{\sigma}^{\text{TOF}} < 3$
Pb–Pb	0.5–1.5	$-1 < n_{\sigma}^{\text{TPC}} < 3$	$ n_{\sigma}^{\text{ITS}} < 1$	$ n_{\sigma}^{\text{TOF}} < 2$
	1.5–3	$0 < n_{\sigma}^{\text{TPC}} < 3$	$ n_{\sigma}^{\text{ITS}} < 2$	$ n_{\sigma}^{\text{TOF}} < 2$

Table 3: Electron identification criteria used in the analyses (see text for more details).

in pp collisions, with negligible dependence on centrality and pseudorapidity. In both collision systems the hadron contamination is subtracted statistically from the inclusive electron candidate yield.

3.2 Subtraction of electrons from non heavy-flavour sources

The raw inclusive sample of electron candidates ($p_T < 3$ GeV/c) consists of the signal, i.e. the electrons from semileptonic heavy-flavour hadron decays, and four background components:

1. photonic electrons from Dalitz decays of light neutral mesons (predominantly π^0 and η mesons) and the conversion of their decay photons in the detector material, as well as from prompt virtual and real photons from thermal and hard scattering processes;
2. electrons from weak $K^{0/\pm} \rightarrow e^{\pm} \pi^{\mp/0} \nu_e^{(-)}$ (K_{e3}) decays;
3. dielectron decays of quarkonia;
4. dielectron decays of light vector mesons.

The photonic-electron tagging method [45, 62] is adopted for the subtraction of the first and main background component. For $p_T < 1.5$ GeV/c the inclusive electron yield is largely dominated by the contribution of photonic electrons. The ratio of the signal to the photonic electron background is measured to be 0.2 at $p_T = 0.5$ GeV/c and it is observed to increase reaching a value of 3 at $p_T = 3$ GeV/c [28]. Photonic electrons originate from electron-positron pairs with a small invariant mass ($m_{e^+e^-}$). They are tagged by pairing an electron (positron) track with opposite charge tracks identified as positrons (electrons) from the same event. The latter are called associated electrons in the following and they are selected with less stringent requirements listed in Table 4. The combinatorial background from uncorrelated electron-positron pairs is subtracted using as a proxy the like-sign invariant mass distribution in the same invariant mass interval. A selection on the pair invariant mass is applied as listed in Table 4.

Due to detector acceptance and inefficiencies and because of the decay kinematics, not all photonic electrons in the inclusive electron sample are tagged with this method. Therefore, the raw yield of tagged photonic electrons is corrected for the efficiency to find the associated electron (positron), hereafter called tagging efficiency. This efficiency is estimated with Monte Carlo (MC) simulations. In particular, HIJING v1.383 [63] was used to simulate Pb–Pb collisions, while the PYTHIA 6 (Perugia 2011 tune) [64] event generator was used for the simulation of pp events. The transport of particles in the detector is performed using GEANT3 [65]. In both analyses, the generated π^0 p_T distributions in MC are weighted so as to match the measured neutral pion p_T spectra [66, 67]. In the pp analysis, the η p_T spectra are weighted using the corresponding measurement [68], while for Pb–Pb collisions the η weights are determined via m_T -scaling of the measured π^0 p_T spectra [69, 70]. The resulting η/π^0 ratios agree within uncertainties with the ratios measured by ALICE in 0-10% and 20-50% central Pb–Pb collisions at $\sqrt{s_{NN}} = 2.76$ TeV [71]. The photonic electron tagging efficiency increases with the electron p_T , starting from a value of $\approx 40\%$ ($\approx 30\%$) at $p_T = 0.5$ GeV/c and reaching a value of $\approx 70\%$ ($\approx 60\%$) at $p_T = 3$ GeV/c for pp (Pb–Pb) collisions.

Associated electron	Pb–Pb	pp
p_T (GeV/c)	> 0.15	> 0.1
$ y $	< 0.9	< 0.8
Number of TPC clusters	≥ 80	≥ 60
Number of ITS hits	≥ 2	≥ 2
DCA _{xy}	< 2.4 cm	< 1 cm
DCA _z	< 3.2 cm	< 2 cm
TPC dE/dx	$ n_{\sigma}^{\text{TPC}} < 3$	$ n_{\sigma}^{\text{TPC}} < 3$
Electron-positron pair		
$m_{e^+e^-}$ (MeV/c ²)	< 70	< 140

Table 4: Selection criteria for tagging photonic electrons in Pb–Pb and pp collisions.

The background contribution of non-photonic electrons from K_{e3} decays and the dielectron decay of J/ψ mesons is subtracted from the fully corrected and normalized electron yield using the so-called cocktail approach in both pp and Pb–Pb collisions [45, 47, 59, 72]. Due to the requirement of hits in both pixel layers, the relative contribution from K_{e3} decays to the electron background is small and it decreases with p_T , with a maximum of about 0.5% at $p_T = 0.5$ GeV/c for both the collision systems. For pp collisions, the contribution of electrons from J/ψ decays is calculated based on a phenomenological interpolation of the J/ψ production cross sections measured at various values of \sqrt{s} as described in [73], and as done in a previous analysis [47]. For Pb–Pb collisions, the p_T -differential J/ψ yield is calculated by multiplying this reference J/ψ cross section in pp collisions with $\langle T_{AA} \rangle$ and the measured nuclear modification factor in Pb–Pb collisions [74, 75]. The contribution of electrons from J/ψ decays is maximal in the interval $2.0 < p_T < 3.0$ GeV/c, with a value of $\approx 3\%$ in pp collisions and of $\approx 5\%$ in central Pb–Pb collisions. At higher p_T and in less central Pb–Pb collisions the background from J/ψ decays decreases. At lower p_T it is negligible. The background from dielectron decays of light vector mesons and other quarkonium states as well as from Dalitz decays of higher mass mesons (ω , η' , ϕ) is negligible as discussed in Ref. [28].

3.3 Correction and normalisation

After the statistical subtraction of the hadron contamination and the background from photonic electrons, the raw yield of electrons and positrons is divided by the number of events analysed (N_{ev}^{MB}), by the value of p_T at the centre of each bin and its width Δp_T , by the width Δy of the covered rapidity interval, by the geometrical acceptance (ϵ^{geo}) times the reconstruction (ϵ^{reco}) and PID efficiencies (ϵ^{PID}) and a factor of two to obtain the charge averaged invariant differential yield

$$\frac{1}{2\pi p_T} \frac{d^2 N^{e^\pm}}{dp_T dy} = \frac{1}{2} \frac{1}{2\pi p_{T,\text{centre}}} \frac{1}{N_{\text{ev}}^{MB}} \frac{1}{\Delta y \Delta p_T} \frac{N_{\text{raw}}^{e^\pm}(p_T)}{(\epsilon^{\text{geo}} \times \epsilon^{\text{reco}} \times \epsilon^{\text{PID}})}. \quad (2)$$

The invariant production cross section in pp collisions is obtained by further multiplying with the minimum-bias trigger cross section for pp collisions at $\sqrt{s} = 2.76$ TeV, $\sigma_{\text{MB}} = (55.4 \pm 1.0)$ mb [76].

The efficiencies are determined using dedicated MC simulations. The reconstruction efficiencies are computed using a heavy-flavour enriched PYTHIA 6 [64] MC sample in which each simulated pp event contains a $c\bar{c}$ or $b\bar{b}$ pair, and heavy-flavour hadrons are forced to decay semi-electronically. In the MC production used for the Pb–Pb analysis the underlying events are simulated using the HIJING v1.383 generator [63] and the heavy-flavour signal from the PYTHIA 6 generator is added. Out of all produced particles in these PYTHIA pp events, only the heavy-flavour decay products are kept and transported through the detector together with the particles produced with HIJING. In order to better reproduce

the experimental conditions for the detector occupancy, the number of heavy quarks injected into each HIJING event is adjusted according to the Pb–Pb collision centrality. In Pb–Pb collisions, the bin-wise total reconstruction efficiencies ($\varepsilon^{\text{geo}} \times \varepsilon^{\text{reco}} \times \varepsilon^{\text{eID}}$) do not show any significant p_T dependence and are about 8% (9%) in the 0–10% (20–40%) centrality class. Due to the less stringent selections applied for pp collisions, the total electron reconstruction efficiency reaches a value of about 27% at $p_T = 3$ GeV/ c in this case. Finally, the remaining background contributions from weak K_{e3} decays and dielectron decays of J/ψ mesons are subtracted from the fully corrected cross section (yield) for pp (Pb–Pb) collisions.

3.4 Systematic uncertainties

The overall systematic uncertainty on the p_T spectra is calculated summing in quadrature the different uncorrelated contributions, which are summarised in Table 5 and discussed in the following.

The systematic uncertainties arising from the residual discrepancy between MC used to determine the total reconstruction efficiency and data is estimated by systematically varying the track selection and PID requirements around the default values chosen in the analysis. The systematic uncertainties are determined as the root mean squared (RMS) of the distribution of the resulting corrected yields (or cross sections in pp) obtained for different selections in each p_T interval, considering also shifts of the mean value with respect to the default selections. In the Pb–Pb analysis, this contribution is about 6% at low p_T ($p_T < 1$ GeV/ c), and it decreases with increasing p_T reaching about 3% at the highest p_T . In the pp case this contribution is about 4% without p_T dependence.

In the pp analysis, a systematic uncertainty of about 2% (3%) is assigned due to the incomplete knowledge of the efficiency in matching tracks reconstructed in the ITS and TPC (TPC and TOF) [47, 59]. In Pb–Pb collisions, the uncertainty assigned on the measurements coming from the track-reconstruction procedure amounts to 5% for single tracks [77].

The solenoid polarity was changed during the Pb–Pb data taking period. From the comparison of the fully corrected spectra of electrons from semileptonic heavy-flavour hadron decays measured in events with the magnetic field oriented in the two opposite directions, a 2% systematic uncertainty is assigned for $p_T \leq 1.25$ GeV/ c . To ensure that the results are not biased by tracks detected at the edges of the detector, where the efficiencies are more difficult to be calculated, the measurements were re-done restricting the rapidity window for the electrons down to $|y| < 0.5$. In addition, possible biases in the efficiency determination are checked by performing the analyses only in the positive or the negative rapidity region. A 5% systematic uncertainty has been estimated for $p_T < 1.5$ GeV/ c in both pp and Pb–Pb collisions.

The systematic uncertainty arising from the photonic-electron subtraction technique is estimated similarly as the RMS of the distribution of yields obtained by varying the selection criteria listed in Table 4. In the Pb–Pb analysis, because of the large combinatorial background of random pairs, this systematic uncertainty is of the order of $\pm 30\%$ in the 0–10% most-central collisions and $\pm 18\%$ in the centrality class 20–40% for the p_T interval 0.5–0.7 GeV/ c . It is observed to decrease with increasing p_T reaching 2% for $p_T = 2$ GeV/ c , where the contribution of background electrons starts to become negligible. In pp collisions, the uncertainty arising from the photonic-electron subtraction is estimated to be about 3% with no p_T dependence. In addition, the dependence of the photonic-electron tagging efficiency on the spectral shape of the background sources is taken into account by recalculating the efficiency for different π^0 and η p_T spectra. The variation of the neutral-meson spectra is obtained by parameterising the measured spectra considering their systematic uncertainties. In particular, the measured yields at the lowest transverse momenta are shifted up by their systematic uncertainties and the yields at the highest transverse momenta are shifted down, and vice versa. The resulting systematic uncertainty on the spectra of electrons from semileptonic heavy-flavour hadron decays is 1% for $p_T \leq 0.9$ GeV/ c in Pb–Pb collisions. In pp collisions, the systematic uncertainty is about 5% in the p_T interval 0.5–0.7 GeV/ c , 2% in 0.7–0.9 GeV/ c , 1% in 0.9–1.5 GeV/ c and negligible for higher p_T . It is worth noting that replacing the previous

approach to determine the photonic background via a cocktail calculation of the known sources [47] by an actual measurement of this background component resulted in a reduction of the related systematic uncertainties of the pp reference cross section by a factor of about 3.

In order to further test the robustness of the photonic-electron tagging, the number of clusters required for electron candidates in the SPD has been released to a single hit in any of the two layers, increasing in this way the fraction of electrons coming from photon conversions in the detector material. In the pp analysis, a contribution to the systematic uncertainties of about 20% in the p_T interval 0.5–0.7 GeV/c and 5% up to $p_T = 1.3$ GeV/c is assigned, while for higher p_T this uncertainty is estimated to be negligible. In the Pb–Pb case the systematic uncertainty is 3% with no p_T and centrality dependence. This systematic uncertainty is significantly larger for the pp sample because of the specific detector configuration. Due to the lack of the SDD detector information at track reconstruction level, only a maximum of four hits in the ITS can be expected instead of the usual six. Therefore, this sample is potentially affected by a higher fraction of badly reconstructed tracks, particularly at the lowest transverse momenta. In addition to releasing the condition on the SPD layers, the systematic uncertainty in the pp case has been determined by comparing the measurement obtained from the analysis of a sub-set of events where all six ITS layers are used for the track reconstruction.

The subtraction of the background electron contribution from the J/ψ and K_{e3} decays is affected by the uncertainty on the input distribution used for the cocktail calculation. This results in an uncertainty of 4% and 2% in the lowest p_T interval in pp and in Pb–Pb collisions, respectively. While for pp collisions this contribution is negligible at higher p_T , for Pb–Pb collisions it decreases slowly with increasing p_T , reaching a minimum of 1% at $p_T = 1.5$ GeV/c before increasing again to 4% at $p_T = 3$ GeV/c due to the growing contribution from J/ψ decays.

Events with a primary vertex reconstructed using charged-particle tracks are used. For the pp analysis, the resolution of the vertex position is affected by the absence of the SDD information and by the lower multiplicity of tracks compared to the Pb–Pb case. The associated uncertainty of 3% is estimated by comparing the cross sections measured from events where the vertex was determined either with charged-particle tracks or with the SPD information only.

Collision system p_T interval (GeV/c)	Pb–Pb (0-10%)		Pb–Pb (20-40%)		pp	
	0.5–0.7	2–3	0.5–0.7	2–3	0.5–0.7	2–3
Electron candidate selection	6%	3%	6%	3%	4%	-
Photonic electron subtraction	30%	2%	18%	2%	3%	-
π^0 and η Weights	1%	-	1%	-	5%	-
SPD requirement	3%	-	3%	-	20%	-
Track matching	5%	-	5%	-	4%	-
Magnet polarity	2%	-	2%	-	-	-
Rapidity range	5%	-	5%	-	5%	-
Event selection	-	-	-	-	3%	-
Subtraction of J/ψ and K_{e3}	2%	4%	2%	3%	4%	-
Total systematic uncertainty	32%	8%	21%	7%	23%	7%

Table 5: Contributions to the systematic uncertainties on the yield of electrons from semileptonic heavy-flavour hadron decays, quoted for the lowest and highest p_T interval, respectively.

4 Results

4.1 p_T -differential invariant cross section in pp collisions

The measurement presented in this paper for pp collisions updates the charge averaged p_T -differential cross section published previously [47] in the range $p_T < 3.0$ GeV/c. The new p_T -differential invariant cross section for electrons from semileptonic heavy-flavour hadron decays measured at mid-rapidity in pp collisions at $\sqrt{s} = 2.76$ TeV is shown in Fig. 1. Results from a previous publication [47] (open circles in Fig. 1) are plotted together with the new results from the TPC-TOF analysis (filled circles in Fig. 1) reported in the current paper. Applying the photonic tagging background subtraction method [45] allowed for a reduction of the systematic uncertainties of the pp reference cross section by a factor of about 3 compared to the previously published reference [47], which is consistent within uncertainties with the current measurement. The cross section from a pQCD calculation employing the Fixed-Order-Next-to-Leading-Log (FONLL) scheme [78] is compared with the data in Fig. 1. The uncertainties of the FONLL calculations (red dashed area) reflect different choices for the charm and beauty quark masses, the factorization and renormalization scales as well as from the uncertainty on the set of parton distribution functions used in the pQCD calculation (CTEQ6.6 [79]). The result from the FONLL calculation is consistent with the measured production cross section of electrons from semileptonic heavy-flavour hadron decays. The measured cross section is close to the upper edge of the FONLL uncertainty band, as it was observed previously in pp collisions at the LHC [47, 59] and at RHIC, for $p_T > 1.5$ GeV/c [23, 24], as well as in $p\bar{p}$ collisions at the Tevatron [80].

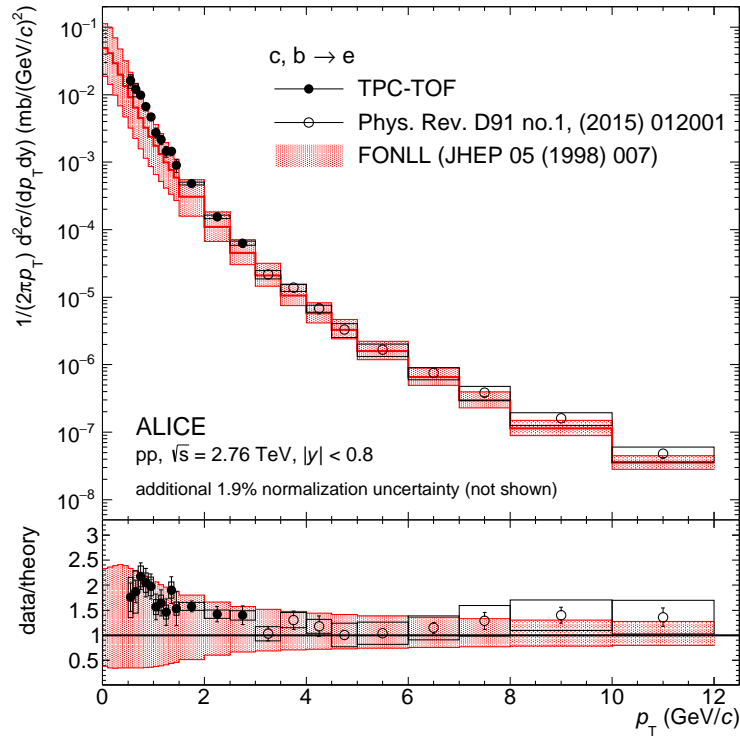


Figure 1: The p_T -differential invariant production cross section for electrons from semileptonic heavy-flavour hadron decays measured at mid-rapidity in pp collisions at $\sqrt{s} = 2.76$ TeV in comparison with FONLL pQCD calculations [78] (upper panel), and the ratio of the data to the FONLL calculation (lower panel). Statistical and systematic uncertainties are shown as vertical bars and boxes, respectively.

4.2 p_T -differential invariant yields in Pb–Pb collisions

The charge averaged p_T -differential invariant yields of electrons and positrons from semileptonic heavy-flavour hadron decays measured in the range $0.5 < p_T < 3$ GeV/ c at mid-rapidity in 0–10% (black circles) and 20–40% (red squares) central Pb–Pb collisions at $\sqrt{s_{NN}} = 2.76$ TeV are depicted in Fig. 2.

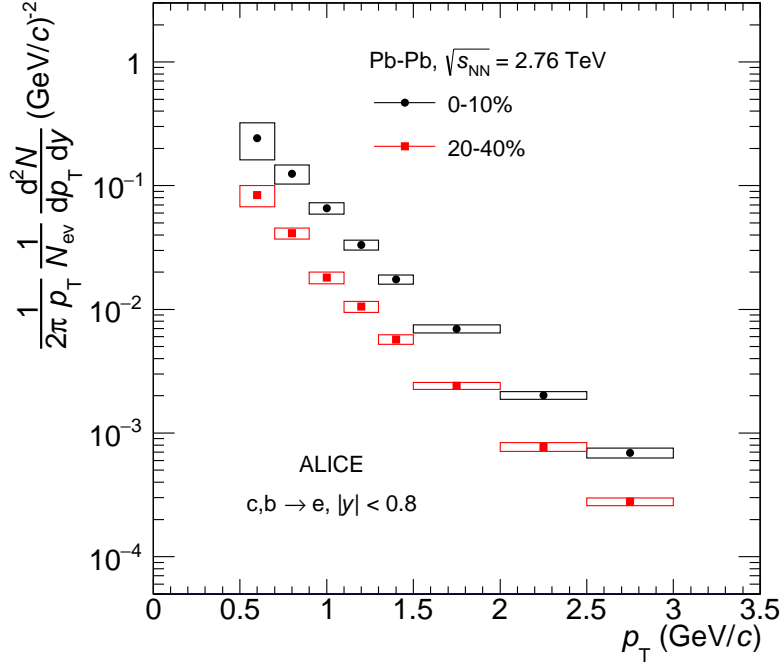


Figure 2: The p_T -differential invariant yields of electrons from semileptonic heavy-flavour hadron decays measured at mid-rapidity in 0–10% and 20–40% central Pb–Pb collisions at $\sqrt{s_{NN}} = 2.76$ TeV. Statistical uncertainties are smaller than the symbol size and the systematic uncertainties are shown as boxes.

4.3 Nuclear modification factor R_{AA}

Figure 3 shows the nuclear modification factor of electrons from semileptonic heavy-flavour hadron decays at mid-rapidity as a function of p_T in Pb–Pb collisions at $\sqrt{s_{NN}} = 2.76$ TeV for the 0–10% (left panel) and 20–40% (right panel) centrality classes. The low- p_T data from the current analysis (filled symbols) are shown together with the previously published [42] high- p_T R_{AA} (open symbols). The 20–30% and 30–40% centrality intervals from [42], in which electrons were identified using the specific energy loss in the TPC and electromagnetic showers reconstructed in the electromagnetic calorimeter (EMCal) of ALICE, have been combined. Statistical and systematic uncertainties of the p_T -differential yields and cross sections in Pb–Pb and pp collisions, respectively, are propagated as uncorrelated uncertainties. The 1.9% normalization uncertainty on the pp measurement is included in the systematic uncertainties of the invariant cross section, and summed in quadrature with the other systematic uncertainties. The uncertainties of the average nuclear overlap function $\langle T_{AA} \rangle$ in the 0–10% and 20–40% centrality classes are represented by the boxes at $R_{AA} = 1$. For $p_T > 3$ GeV/ c the yield of electrons from heavy-flavour hadron decays is suppressed strongly which was interpreted as due to partonic energy loss in the QGP produced in Pb–Pb collisions [42]. The current measurement provides an extension of the p_T coverage to lower values, *i.e.* from $p_T = 3$ GeV/ c down to 0.5 GeV/ c . In this region, the suppression of the yield of electrons from heavy-flavour hadron decays is expected to decrease with decreasing p_T as a consequence of the scaling of the total heavy-flavour yield with the number of binary collisions in Pb–Pb collisions. This scaling, however can be broken due to the nuclear modification of the parton distribution functions in Pb-nuclei, leading to p_T -integrated R_{AA} of less than one. Moreover, further modifications of the p_T distribution due to the radial flow can also play a role in this region. The observed R_{AA} in Fig. 3 is consistent with the

expectation of an increasing R_{AA} with decreasing p_T , reaching values close to unity within uncertainties. However the current uncertainties are still too large to quantify the different effects. Within the current statistical and systematic uncertainties, no significant centrality dependence is observed in the p_T -region below 3 GeV/c.

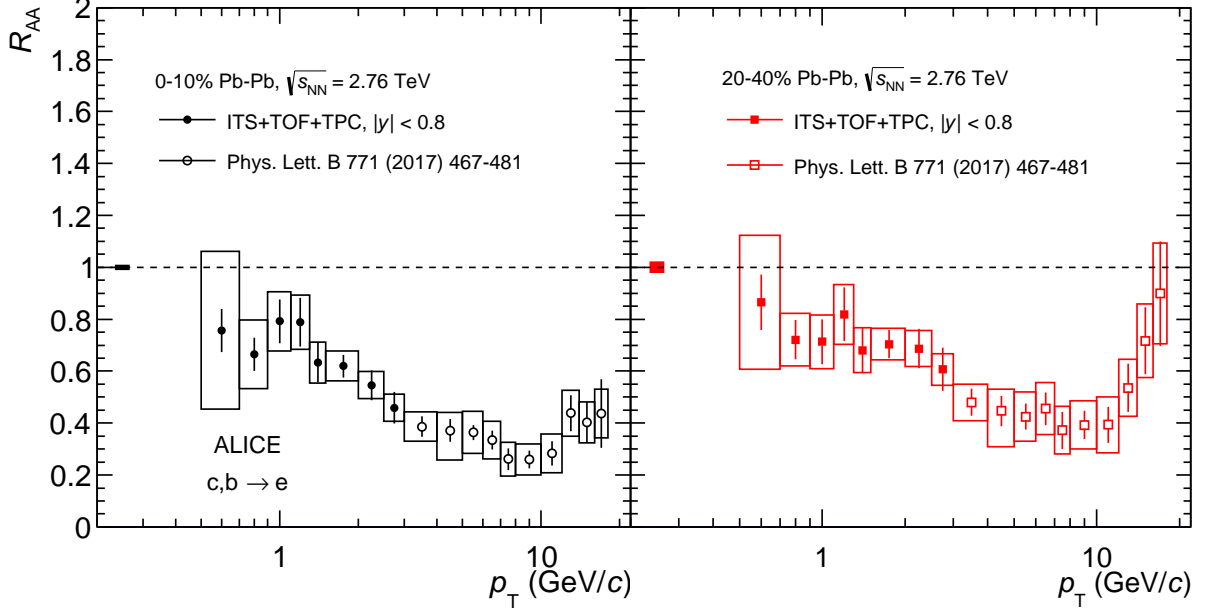


Figure 3: Nuclear modification factor R_{AA} for electrons from semileptonic heavy-flavour hadron decays at mid-rapidity as a function of p_T in 0–10% (left panel) and 20–40% central (right panel) Pb–Pb collisions at $\sqrt{s_{NN}} = 2.76$ TeV. Error bars (open boxes) represent the statistical (systematic) uncertainties. The normalization uncertainties are represented by the boxes at $R_{AA} = 1$. The previously published results from [42] have been updated using a new glauber model calculation [60].

5 Comparison with model calculations

In Fig. 4 results from model calculations including charm and beauty quark interactions with a QGP medium [81–86] are compared with the measured R_{AA} of electrons from semileptonic heavy-flavour hadron decays for the 10% most central Pb–Pb collisions. The calculations differ in the modelling of the initial conditions, the medium properties, the dynamics of the medium evolution, the interactions of charm and beauty quarks with the QGP, and in the implementation of hadronisation and hadronic interactions in the late stages of the heavy-ion collision. Furthermore, there are differences in the initial p_T -differential heavy-quark production cross section in nucleon-nucleon collisions used as input. Qualitatively, most models provide a good description of the heavy-flavour R_{AA} measured in the most central Pb–Pb collisions as already observed for D mesons [42].

The measurement presented in this paper shows for the first time electrons from heavy-flavour hadron decays in the p_T interval below 1 GeV/c, where decays of heavy-flavour hadrons down to zero p_T contribute. In this region, the nuclear modifications of the PDFs can play a significant role [39–42]. This is addressed in Fig. 5, which compares the measured nuclear modification factor with TAMU, POWLANG and MC@sHQ+EPOS2 model calculations with and without the inclusion of the EPS09 shadowing parameterisations [34]. The depletion of the parton densities at low x , resulting in a reduced heavy-flavour production cross section per nucleon-nucleon pair in Pb–Pb collisions with respect to bare nucleon–nucleon collisions, leads to a reduction of R_{AA} of electrons from heavy-flavour hadron decays at low

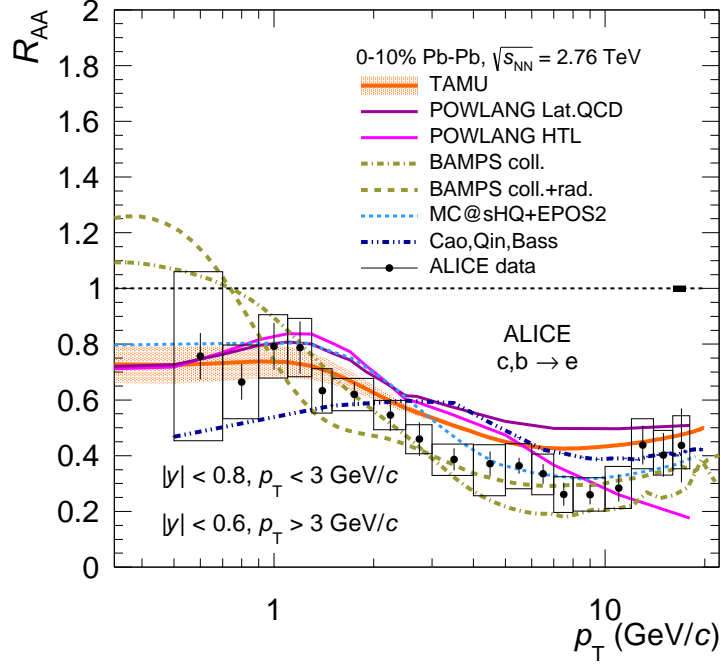


Figure 4: R_{AA} of electrons from semileptonic heavy-flavour hadron decays at mid-rapidity as a function of p_T in 0–10% Pb–Pb collisions at $\sqrt{s_{NN}} = 2.76$ TeV compared to model calculations [81–86].

p_T . Data are better described when the nuclear PDFs are included in the theoretical calculation in both centrality intervals. However, the experimental uncertainties are still too large to provide quantitative constraints on the nuclear shadowing contribution. A similar conclusion arises from measurements of D-meson production in Pb–Pb collisions [43].

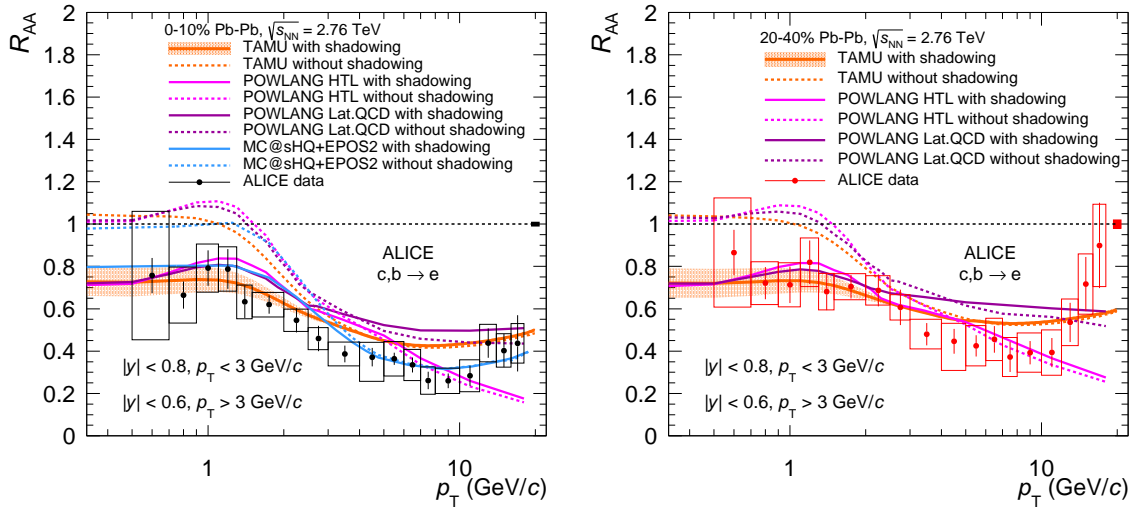


Figure 5: R_{AA} of electrons from semileptonic heavy-flavour hadron decays at mid-rapidity as a function of p_T in 0–10% (left) and 20–40% central (right) Pb–Pb collisions at $\sqrt{s_{NN}} = 2.76$ TeV compared to model calculations [83] with and without EPS09 shadowing parameterisations [34].

6 Conclusions

The production of electrons from semileptonic decays of heavy-flavour hadrons has been measured at mid-rapidity ($|y| < 0.8$) in the p_T interval 0.5-3 GeV/ c in pp collisions and in 0–10% and 20–40% central Pb–Pb collisions at a centre-of-mass energy of 2.76 TeV per nucleon pair. The dominant background from photonic electron sources has been measured and subtracted via the photonic-electron tagging technique for the first time in pp and Pb–Pb collisions at the same energy. The systematic uncertainties have been substantially reduced (up to a factor 3), and the p_T coverage has been extended to lower values with respect to previously published ALICE measurements.

The measured nuclear modification factor R_{AA} of electrons from semileptonic heavy-flavour hadron decays confirms the strong suppression of high- p_T heavy-flavour hadrons in central Pb–Pb collisions with respect to the binary-collision scaled pp reference, consistent with previous observations in various heavy-flavour channels. With decreasing p_T , R_{AA} grows approaching values close to unity, as expected from the hypothesis of the binary-collision scaling for the total heavy-quark yield. However, this kinematic region is sensitive to the effects of nuclear shadowing: the depletion of parton densities in nuclei at low Bjorken x values can reduce the heavy-quark production cross section per binary collision in Pb–Pb with respect to the pp case. This initial-state effect is studied in p–Pb collisions [45]. However, the present uncertainties on the R_{pPb} measurement do not allow quantitative conclusions on the modification of the PDF in nuclei in the low p_T region. With the improved precision of the results presented here, the Pb–Pb data exhibit their sensitivity to the modification of the PDF in nuclei, like nuclear shadowing, at low p_T . The measured R_{AA} is in better agreement with TAMU and POWLANG model calculations when the nuclear modification of the PDF is included.

Acknowledgements

The ALICE Collaboration would like to thank all its engineers and technicians for their invaluable contributions to the construction of the experiment and the CERN accelerator teams for the outstanding performance of the LHC complex. The ALICE Collaboration gratefully acknowledges the resources and support provided by all Grid centres and the Worldwide LHC Computing Grid (WLCG) collaboration. The ALICE Collaboration acknowledges the following funding agencies for their support in building and running the ALICE detector: A. I. Alikhanyan National Science Laboratory (Yerevan Physics Institute) Foundation (ANSL), State Committee of Science and World Federation of Scientists (WFS), Armenia; Austrian Academy of Sciences and Nationalstiftung für Forschung, Technologie und Entwicklung, Austria; Ministry of Communications and High Technologies, National Nuclear Research Center, Azerbaijan; Conselho Nacional de Desenvolvimento Científico e Tecnológico (CNPq), Universidade Federal do Rio Grande do Sul (UFRGS), Financiadora de Estudos e Projetos (Finep) and Fundação de Amparo à Pesquisa do Estado de São Paulo (FAPESP), Brazil; Ministry of Science & Technology of China (MSTC), National Natural Science Foundation of China (NSFC) and Ministry of Education of China (MOEC), China; Ministry of Science and Education, Croatia; Ministry of Education, Youth and Sports of the Czech Republic, Czech Republic; The Danish Council for Independent Research — Natural Sciences, the Carlsberg Foundation and Danish National Research Foundation (DNRF), Denmark; Helsinki Institute of Physics (HIP), Finland; Commissariat à l’Energie Atomique (CEA) and Institut National de Physique Nucléaire et de Physique des Particules (IN2P3) and Centre National de la Recherche Scientifique (CNRS), France; Bundesministerium für Bildung, Wissenschaft, Forschung und Technologie (BMBF) and GSI Helmholtzzentrum für Schwerionenforschung GmbH, Germany; General Secretariat for Research and Technology, Ministry of Education, Research and Religions, Greece; National Research, Development and Innovation Office, Hungary; Department of Atomic Energy Government of India (DAE), Department of Science and Technology, Government of India (DST), University Grants Commission, Government of India (UGC) and Council of Scientific and Industrial Research (CSIR), India; Indonesian Institute of Science, Indonesia; Centro Fermi - Museo Storico della Fisica e Centro Studi

e Ricerche Enrico Fermi and Istituto Nazionale di Fisica Nucleare (INFN), Italy; Institute for Innovative Science and Technology, Nagasaki Institute of Applied Science (IIST), Japan Society for the Promotion of Science (JSPS) KAKENHI and Japanese Ministry of Education, Culture, Sports, Science and Technology (MEXT), Japan; Consejo Nacional de Ciencia (CONACYT) y Tecnología, through Fondo de Cooperación Internacional en Ciencia y Tecnología (FONCICYT) and Dirección General de Asuntos del Personal Académico (DGAPA), Mexico; Nederlandse Organisatie voor Wetenschappelijk Onderzoek (NWO), Netherlands; The Research Council of Norway, Norway; Commission on Science and Technology for Sustainable Development in the South (COMSATS), Pakistan; Pontificia Universidad Católica del Perú, Peru; Ministry of Science and Higher Education and National Science Centre, Poland; Korea Institute of Science and Technology Information and National Research Foundation of Korea (NRF), Republic of Korea; Ministry of Education and Scientific Research, Institute of Atomic Physics and Romanian National Agency for Science, Technology and Innovation, Romania; Joint Institute for Nuclear Research (JINR), Ministry of Education and Science of the Russian Federation and National Research Centre Kurchatov Institute, Russia; Ministry of Education, Science, Research and Sport of the Slovak Republic, Slovakia; National Research Foundation of South Africa, South Africa; Centro de Aplicaciones Tecnológicas y Desarrollo Nuclear (CEADEN), Cubaenergía, Cuba and Centro de Investigaciones Energéticas, Medioambientales y Tecnológicas (CIEMAT), Spain; Swedish Research Council (VR) and Knut & Alice Wallenberg Foundation (KAW), Sweden; European Organization for Nuclear Research, Switzerland; National Science and Technology Development Agency (NSDTA), Suranaree University of Technology (SUT) and Office of the Higher Education Commission under NRU project of Thailand, Thailand; Turkish Atomic Energy Agency (TAEK), Turkey; National Academy of Sciences of Ukraine, Ukraine; Science and Technology Facilities Council (STFC), United Kingdom; National Science Foundation of the United States of America (NSF) and United States Department of Energy, Office of Nuclear Physics (DOE NP), United States of America.

References

- [1] **BRAHMS** Collaboration, I. Arsene *et al.*, “Quark gluon plasma and color glass condensate at RHIC? The Perspective from the BRAHMS experiment,” *Nucl. Phys.* **A757** (2005) 1–27, arXiv:nucl-ex/0410020 [nucl-ex].
- [2] **PHENIX** Collaboration, K. Adcox *et al.*, “Formation of dense partonic matter in relativistic nucleus-nucleus collisions at RHIC: Experimental evaluation by the PHENIX collaboration,” *Nucl. Phys.* **A757** (2005) 184–283, arXiv:nucl-ex/0410003 [nucl-ex].
- [3] B. B. Back *et al.*, “The PHOBOS perspective on discoveries at RHIC,” *Nucl. Phys.* **A757** (2005) 28–101, arXiv:nucl-ex/0410022 [nucl-ex].
- [4] **STAR** Collaboration, J. Adams *et al.*, “Experimental and theoretical challenges in the search for the quark gluon plasma: The STAR Collaboration’s critical assessment of the evidence from RHIC collisions,” *Nucl. Phys.* **A757** (2005) 102–183, arXiv:nucl-ex/0501009 [nucl-ex].
- [5] **ALICE** Collaboration, K. Aamodt *et al.*, “Elliptic flow of charged particles in Pb-Pb collisions at 2.76 TeV,” *Phys. Rev. Lett.* **105** (2010) 252302, arXiv:1011.3914 [nucl-ex].
- [6] **ALICE** Collaboration, K. Aamodt *et al.*, “Suppression of Charged Particle Production at Large Transverse Momentum in Central Pb-Pb Collisions at $\sqrt{s_{NN}} = 2.76$ TeV,” *Phys. Lett.* **B696** (2011) 30–39, arXiv:1012.1004 [nucl-ex].
- [7] F. Karsch, “Lattice simulations of the thermodynamics of strongly interacting elementary particles and the exploration of new phases of matter in relativistic heavy ion collisions,” *J. Phys. Conf. Ser.* **46** (2006) 122–131, arXiv:hep-lat/0608003 [hep-lat].

- [8] **Wuppertal-Budapest** Collaboration, S. Borsanyi, Z. Fodor, C. Hoelbling, S. D. Katz, S. Krieg, C. Ratti, and K. K. Szabo, “Is there still any T_c mystery in lattice QCD? Results with physical masses in the continuum limit III,” *JHEP* **09** (2010) 073, arXiv:1005.3508 [hep-lat].
- [9] **Wuppertal-Budapest** Collaboration, S. Borsanyi, G. Endrodi, Z. Fodor, A. Jakovac, S. D. Katz, S. Krieg, C. Ratti, and K. K. Szabo, “The QCD equation of state with dynamical quarks,” *JHEP* **11** (2010) 077, arXiv:1007.2580 [hep-lat].
- [10] A. Bazavov *et al.*, “The chiral and deconfinement aspects of the QCD transition,” *Phys. Rev.* **D85** (2012) 054503, arXiv:1111.1710 [hep-lat].
- [11] P. Petreczky, “Review of recent highlights in lattice calculations at finite temperature and finite density,” *PoS ConfinementX* (2012) 028, arXiv:1301.6188 [hep-lat].
- [12] F.-M. Liu and S.-X. Liu, “Quark-gluon plasma formation time and direct photons from heavy ion collisions,” *Phys. Rev.* **C89** no. 3, (2014) 034906, arXiv:1212.6587 [nucl-th].
- [13] R. Averbek, “Heavy-flavor production in heavy-ion collisions and implications for the properties of hot QCD matter,” *Prog. Part. Nucl. Phys.* **70** (2013) 159–209, arXiv:1505.03828 [nucl-ex].
- [14] F. Prino and R. Rapp, “Open Heavy Flavor in QCD Matter and in Nuclear Collisions,” *J. Phys.* **G43** no. 9, (2016) 093002, arXiv:1603.00529 [nucl-ex].
- [15] P. Braun-Munzinger, “Quarkonium production in ultra-relativistic nuclear collisions: Suppression versus enhancement,” *J. Phys.* **G34** (2007) S471–478, arXiv:nucl-th/0701093 [NUCL-TH].
- [16] R. Glauber and G. Matthiae, “High-energy scattering of protons by nuclei,” *Nucl. Phys.* **B21** (1970) 135–157.
- [17] M. L. Miller, K. Reygers, S. J. Sanders, and P. Steinberg, “Glauber modeling in high energy nuclear collisions,” *Ann. Rev. Nucl. Part. Sci.* **57** (2007) 205–243, arXiv:nucl-ex/0701025 [nucl-ex].
- [18] M. Gyulassy and M. Plumer, “Jet Quenching in Dense Matter,” *Phys. Lett.* **B243** (1990) 432–438.
- [19] R. Baier, Y. L. Dokshitzer, A. H. Mueller, S. Peigne, and D. Schiff, “Radiative energy loss and p_T -broadening of high-energy partons in nuclei,” *Nucl. Phys.* **B484** (1997) 265–282, arXiv:hep-ph/9608322 [hep-ph].
- [20] M. H. Thoma and M. Gyulassy, “Quark damping and energy loss in the high temperature QCD,” *Nuclear Physics B* **351** no. 3, (1991) 491 – 506.
<http://www.sciencedirect.com/science/article/pii/S0550321305800318>.
- [21] E. Braaten and M. H. Thoma, “Energy loss of a heavy fermion in a hot QED plasma,” *Phys. Rev. D* **44** (Aug, 1991) 1298–1310.
<http://link.aps.org/doi/10.1103/PhysRevD.44.1298>.
- [22] E. Braaten and M. H. Thoma, “Energy loss of a heavy quark in the quark-gluon plasma,” *Phys. Rev. D* **44** (Nov, 1991) R2625–R2630.
<http://link.aps.org/doi/10.1103/PhysRevD.44.R2625>.
- [23] **STAR** Collaboration, B. I. Abelev *et al.*, “Transverse momentum and centrality dependence of high- p_T non-photon electron suppression in Au+Au collisions at $\sqrt{s_{NN}} = 200$ GeV,” *Phys. Rev. Lett.* **98** (2007) 192301, arXiv:nucl-ex/0607012 [nucl-ex]. [Erratum: *Phys. Rev. Lett.* 106,159902(2011)].

- [24] **PHENIX** Collaboration, A. Adare *et al.*, “Heavy Quark Production in pp and Energy Loss and Flow of Heavy Quarks in Au–Au Collisions at $\sqrt{s_{NN}}=200$ GeV,” *Phys. Rev.* **C84** (2011) 044905, arXiv:1005.1627 [nucl-ex].
- [25] **PHENIX** Collaboration, S. S. Adler *et al.*, “Nuclear modification of electron spectra and implications for heavy quark energy loss in Au+Au collisions at $\sqrt{s_{NN}}=200$ GeV,” *Phys. Rev. Lett.* **96** (2006) 032301, arXiv:nucl-ex/0510047 [nucl-ex].
- [26] **PHENIX** Collaboration, A. Adare *et al.*, “System-size dependence of open-heavy-flavor production in nucleus-nucleus collisions at $\sqrt{s_{NN}} = 200$ GeV,” *Phys. Rev.* **C90** no. 3, (2014) 034903, arXiv:1310.8286 [nucl-ex].
- [27] **STAR** Collaboration, L. Adamczyk *et al.*, “Observation of D^0 Meson Nuclear Modifications in Au+Au Collisions at $\sqrt{s_{NN}} = 200$ GeV,” *Phys. Rev. Lett.* **113** no. 14, (2014) 142301, arXiv:1404.6185 [nucl-ex].
- [28] **ALICE** Collaboration, J. Adam *et al.*, “Elliptic flow of electrons from heavy-flavour hadron decays at mid-rapidity in Pb–Pb collisions at $\sqrt{s_{NN}} = 2.76$ TeV,” *JHEP* **09** (2016) 028, arXiv:1606.00321 [nucl-ex].
- [29] **ALICE** Collaboration, B. Abelev *et al.*, “D meson elliptic flow in non-central Pb–Pb collisions at $\sqrt{s_{NN}} = 2.76$ TeV,” *Phys. Rev. Lett.* **111** (2013) 102301, arXiv:1305.2707 [nucl-ex].
- [30] H. van Hees, V. Greco, and R. Rapp, “Heavy-quark probes of the quark-gluon plasma at RHIC,” *Phys. Rev.* **C73** (2006) 034913, arXiv:nucl-th/0508055 [nucl-th].
- [31] V. Greco, C. M. Ko, and R. Rapp, “Quark coalescence for charmed mesons in ultrarelativistic heavy ion collisions,” *Phys. Lett.* **B595** (2004) 202–208, arXiv:nucl-th/0312100 [nucl-th].
- [32] A. Andronic, P. Braun-Munzinger, K. Redlich, and J. Stachel, “Statistical hadronization of charm in heavy ion collisions at SPS, RHIC and LHC,” *Phys. Lett.* **B571** (2003) 36–44, arXiv:nucl-th/0303036 [nucl-th].
- [33] A. Andronic *et al.*, “Heavy-flavour and quarkonium production in the LHC era: from proton–proton to heavy-ion collisions,” *Eur. Phys. J.* **C76** no. 3, (2016) 107, arXiv:1506.03981 [nucl-ex].
- [34] K. J. Eskola, H. Paukkunen, and C. A. Salgado, “EPS09: A New Generation of NLO and LO Nuclear Parton Distribution Functions,” *JHEP* **04** (2009) 065, arXiv:0902.4154 [hep-ph].
- [35] B. Z. Kopeliovich, J. Nemchik, A. Schafer, and A. V. Tarasov, “Cronin effect in hadron production off nuclei,” *Phys. Rev. Lett.* **88** (2002) 232303, arXiv:hep-ph/0201010 [hep-ph].
- [36] **CMS** Collaboration, A. M. Sirunyan *et al.*, “Nuclear modification factor of D^0 mesons in Pb–Pb collisions at $\sqrt{s_{NN}} = 5.02$ TeV,” arXiv:1708.04962 [nucl-ex].
- [37] **CMS** Collaboration, A. M. Sirunyan *et al.*, “Measurement of the B^\pm Meson Nuclear Modification Factor in Pb–Pb Collisions at $\sqrt{s_{NN}} = 5.02$ TeV,” *Phys. Rev. Lett.* **119** no. 15, (2017) 152301, arXiv:1705.04727 [hep-ex].
- [38] **ALICE** Collaboration, J. Adam *et al.*, “Measurement of electrons from beauty-hadron decays in p–Pb collisions at $\sqrt{s_{NN}} = 5.02$ TeV and Pb–Pb collisions at $\sqrt{s_{NN}} = 2.76$ TeV,” *JHEP* **07** (2017) 052, arXiv:1609.03898 [nucl-ex].

- [39] ALICE Collaboration, B. Abelev *et al.*, “Suppression of high transverse momentum D mesons in central Pb–Pb collisions at $\sqrt{s_{NN}} = 2.76$ TeV,” *JHEP* **09** (2012) 112, arXiv:1203.2160 [nucl-ex].
- [40] ALICE Collaboration, J. Adam *et al.*, “Centrality dependence of high- p_T D meson suppression in Pb–Pb collisions at $\sqrt{s_{NN}} = 2.76$ TeV,” *JHEP* **11** (2015) 205, arXiv:1506.06604 [nucl-ex].
- [41] ALICE Collaboration, B. Abelev *et al.*, “Production of muons from heavy flavour decays at forward rapidity in pp and Pb–Pb collisions at $\sqrt{s_{NN}} = 2.76$ TeV,” *Phys. Rev. Lett.* **109** (2012) 112301, arXiv:1205.6443 [hep-ex].
- [42] ALICE Collaboration, J. Adam *et al.*, “Measurement of the production of high- p_T electrons from heavy-flavour hadron decays in Pb-Pb collisions at $\sqrt{s_{NN}} = 2.76$ TeV,” *Phys. Lett.* **B771** (2017) 467–481, arXiv:1609.07104 [nucl-ex].
- [43] ALICE Collaboration, J. Adam *et al.*, “Transverse momentum dependence of D-meson production in Pb-Pb collisions at $\sqrt{s_{NN}} = 2.76$ TeV,” *JHEP* **03** (2016) 081, arXiv:1509.06888 [nucl-ex].
- [44] CMS Collaboration, V. Khachatryan *et al.*, “Study of B Meson Production in p+Pb Collisions at $\sqrt{s_{NN}} = 5.02$ TeV Using Exclusive Hadronic Decays,” *Phys. Rev. Lett.* **116** no. 3, (2016) 032301, arXiv:1508.06678 [nucl-ex].
- [45] ALICE Collaboration, J. Adam *et al.*, “Measurement of electrons from heavy-flavour hadron decays in p-Pb collisions at $\sqrt{s_{NN}} = 5.02$ TeV,” *Phys. Lett.* **B754** (2016) 81–93, arXiv:1509.07491 [nucl-ex].
- [46] ALICE Collaboration, B. B. Abelev *et al.*, “Measurement of prompt D-meson production in p – Pb collisions at $\sqrt{s_{NN}} = 5.02$ TeV,” *Phys. Rev. Lett.* **113** no. 23, (2014) 232301, arXiv:1405.3452 [nucl-ex].
- [47] ALICE Collaboration, B. B. Abelev *et al.*, “Measurement of electrons from semileptonic heavy-flavor hadron decays in pp collisions at $\sqrt{s} = 2.76$ TeV,” *Phys. Rev.* **D91** no. 1, (2015) 012001, arXiv:1405.4117 [nucl-ex].
- [48] ATLAS Collaboration, “Measurement of the suppression and elliptic anisotropy of heavy flavor muons in Pb+Pb collisions at $\sqrt{s_{NN}} = 2.76$ TeV with the ATLAS detector,” *ATLAS-CONF-2015-053* (2015) .
- [49] ALICE Collaboration, K. Aamodt *et al.*, “The ALICE experiment at the CERN LHC,” *Journal of Instrumentation* **3** no. 08, (2008) S08002. <http://stacks.iop.org/1748-0221/3/i=08/a=S08002>.
- [50] ALICE Collaboration, B. B. Abelev *et al.*, “Performance of the ALICE Experiment at the CERN LHC,” *Int.J.Mod.Phys.* **A29** (2014) 1430044, arXiv:1402.4476 [nucl-ex].
- [51] ALICE Collaboration, K. Aamodt *et al.*, “Alignment of the ALICE Inner Tracking System with cosmic-ray tracks,” *JINST* **5** (2010) P03003, arXiv:1001.0502 [physics.ins-det].
- [52] ALICE Collaboration, J. Alme, Y. Andres, H. Appelshäuser, S. Bablok, N. Bialas, *et al.*, “The ALICE TPC, a large 3-dimensional tracking device with fast readout for ultra-high multiplicity events,” *Nucl.Instrum.Meth.* **A622** (2010) 316–367, arXiv:1001.1950 [physics.ins-det].
- [53] ALICE Collaboration, A. Akindinov *et al.*, “Performance of the ALICE Time-Of-Flight detector at the LHC,” *The European Physical Journal Plus* **128** no. 4, (2013) . <http://dx.doi.org/10.1140/epjp/i2013-13044-x>.

- [54] **ALICE** Collaboration, E. Abbas *et al.*, “Performance of the ALICE VZERO system,” *JINST* **8** (2013) P10016, arXiv:1306.3130 [nucl-ex].
- [55] **ALICE** Collaboration, B. Abelev *et al.*, “Centrality determination of Pb-Pb collisions at $\sqrt{s_{NN}} = 2.76$ TeV with ALICE,” *Phys. Rev.* **C88** no. 4, (2013) 044909, arXiv:1301.4361 [nucl-ex].
- [56] C. Loizides, J. Nagle, and P. Steinberg, “Improved version of the PHOBOS Glauber Monte Carlo,” *SoftwareX* **1-2** (2015) 13–18, arXiv:1408.2549 [nucl-ex].
- [57] B. Alver, M. Baker, C. Loizides, and P. Steinberg, “The PHOBOS Glauber Monte Carlo,” arXiv:0805.4411 [nucl-ex].
- [58] **ALICE** Collaboration, R. Arnaldi *et al.*, “Performance of a forward hadron calorimeter for the alic experiment,” *Nuclear Science Symposium, 1998. Conference Record. 1998 IEEE* **1** (1998) 8–11 vol.1. <http://cds.cern.ch/record/409740>.
- [59] **ALICE** Collaboration, B. Abelev *et al.*, “Measurement of electrons from semileptonic heavy-flavour hadron decays in pp collisions at $\sqrt{s} = 7$ TeV,” *Phys. Rev.* **D86** (2012) 112007, arXiv:1205.5423 [hep-ex].
- [60] **ALICE** Collaboration, “Centrality determination in heavy ion collisions,” *ALICE-PUBLIC-2018-011* (2018) .
- [61] H. Bethe, “Zur Theorie des Durchgangs schneller Korpuskularstrahlen durch Materie,” *Annalen der Physik* **397** no. 3, (1930) 325–400. <http://dx.doi.org/10.1002/andp.19303970303>.
- [62] **STAR** Collaboration, L. Adamczyk *et al.*, “Elliptic flow of electrons from heavy-flavor hadron decays in Au + Au collisions at $\sqrt{s_{NN}} = 200, 62.4,$ and 39 GeV,” *Phys. Rev.* **C95** no. 3, (2017) 034907, arXiv:1405.6348 [hep-ex].
- [63] M. Gyulassy and X. N. Wang, “HIJING 1.0: A Monte Carlo program for parton and particle production in high-energy hadronic and nuclear collisions,” *Comput. Phys. Commun.* **83** (1994) 307.
- [64] T. Sjostrand, S. Mrenna, and P. Z. Skands, “PYTHIA 6.4 Physics and Manual,” *JHEP* **05** (2006) 026, arXiv:hep-ph/0603175 [hep-ph].
- [65] R. Brun, F. Carminati, and S. Giani, “GEANT Detector Description and Simulation Tool,” <http://inspirehep.net/record/863473?ln=en>.
- [66] **ALICE** Collaboration, B. B. Abelev *et al.*, “Neutral pion production at midrapidity in pp and Pb–Pb collisions at $\sqrt{s_{NN}} = 2.76$ TeV,” *Eur. Phys. J.* **C74** no. 10, (2014) 3108, arXiv:1405.3794 [nucl-ex].
- [67] **ALICE** Collaboration, B. B. Abelev *et al.*, “Production of charged pions, kaons and protons at large transverse momenta in pp and Pb–Pb collisions at $\sqrt{s_{NN}} = 2.76$ TeV,” *Phys. Lett.* **B736** (2014) 196–207, arXiv:1401.1250 [nucl-ex].
- [68] **ALICE** Collaboration, S. Acharya *et al.*, “Production of π^0 and η mesons up to high transverse momentum in pp collisions at 2.76 TeV,” *Eur. Phys. J.* **C77** no. 5, (2017) 339, arXiv:1702.00917 [hep-ex]. [*Eur. Phys. J.*C77,no.9,586(2017)].
- [69] **WA80** Collaboration, R. Albrecht *et al.*, “Production of Eta-mesons in 200-A/GeV S + S and S + Au reactions,” *Phys. Lett.* **B361** (1995) 14–20, arXiv:hep-ex/9507009 [hep-ex].

- [70] P. K. Khandai, P. Shukla, and V. Singh, “Meson spectra and m_T scaling in $p + p$, $d + Au$, and $Au + Au$ collisions at $\sqrt{s_{NN}} = 200$ GeV,” *Phys. Rev.* **C84** (2011) 054904, arXiv:1110.3929 [hep-ph].
- [71] ALICE Collaboration, S. Acharya *et al.*, “Neutral pion and η meson production at mid-rapidity in Pb-Pb collisions at $\sqrt{s_{NN}} = 2.76$ TeV,” arXiv:1803.05490 [nucl-ex].
- [72] PHENIX Collaboration, A. Adare *et al.*, “Heavy Quark Production in pp and Energy Loss and Flow of Heavy Quarks in Au–Au Collisions at $\sqrt{s_{NN}} = 200$ GeV,” *Phys.Rev.* **C84** (2011) 044905, arXiv:1005.1627 [nucl-ex].
- [73] F. Bossu, Z. C. del Valle, A. de Falco, M. Gagliardi, S. Grigoryan, and G. Martinez Garcia, “Phenomenological interpolation of the inclusive J/psi cross section to proton-proton collisions at 2.76 TeV and 5.5 TeV,” arXiv:1103.2394 [nucl-ex].
- [74] ALICE Collaboration, J. Adam *et al.*, “Inclusive, prompt and non-prompt J/ψ production at mid-rapidity in Pb-Pb collisions at $\sqrt{s_{NN}} = 2.76$ TeV,” *JHEP* **07** (2015) 051, arXiv:1504.07151 [nucl-ex].
- [75] ALICE Collaboration, J. Adam *et al.*, “ J/ψ suppression at forward rapidity in Pb-Pb collisions at $\sqrt{s_{NN}} = 5.02$ TeV,” *Phys. Lett.* **B766** (2017) 212–224, arXiv:1606.08197 [nucl-ex].
- [76] ALICE Collaboration, B. Abelev *et al.*, “Measurement of inelastic, single- and double-diffraction cross sections in proton–proton collisions at the LHC with ALICE,” *Eur. Phys. J.* **C73** no. 6, (2013) 2456, arXiv:1208.4968 [hep-ex].
- [77] ALICE Collaboration, B. Abelev *et al.*, “Centrality Dependence of Charged Particle Production at Large Transverse Momentum in Pb–Pb Collisions at $\sqrt{s_{NN}} = 2.76$ TeV,” *Phys. Lett.* **B720** (2013) 52–62, arXiv:1208.2711 [hep-ex].
- [78] M. Cacciari, M. Greco, and P. Nason, “The p_T spectrum in heavy flavor hadroproduction,” *JHEP* **05** (1998) 007, arXiv:hep-ph/9803400 [hep-ph].
- [79] P. M. Nadolsky, H.-L. Lai, Q.-H. Cao, J. Huston, J. Pumplin, D. Stump, W.-K. Tung, and C. P. Yuan, “Implications of CTEQ global analysis for collider observables,” *Phys. Rev.* **D78** (2008) 013004, arXiv:0802.0007 [hep-ph].
- [80] CDF II Collaboration Collaboration, “Measurement of prompt charm meson production cross sections in $p\bar{p}$ collisions at $\sqrt{s} = 1.96$ TeV,” *Phys. Rev. Lett.* **91** (Dec, 2003) 241804. <https://link.aps.org/doi/10.1103/PhysRevLett.91.241804>.
- [81] J. Uphoff, O. Fochler, Z. Xu, and C. Greiner, “Open Heavy Flavor in Pb–Pb Collisions at $\sqrt{s_{NN}} = 2.76$ TeV within a Transport Model,” *Phys.Lett.* **B717** (2012) 430–435, arXiv:1205.4945 [hep-ph].
- [82] J. Uphoff, O. Fochler, Z. Xu, and C. Greiner, “Heavy vs. light flavor energy loss within a partonic transport model,” *J.Phys.Conf.Ser.* **509** (2014) 012077, arXiv:1310.3597 [hep-ph].
- [83] M. He, R. J. Fries, and R. Rapp, “Heavy Flavor at the Large Hadron Collider in a Strong Coupling Approach,” *Phys.Lett.* **B735** (2014) 445–450, arXiv:1401.3817 [nucl-th].
- [84] W. Alberico, A. Beraudo, A. De Pace, A. Molinari, M. Monteno, *et al.*, “Heavy flavors in AA collisions: production, transport and final spectra,” *Eur.Phys.J.* **C73** (2013) 2481, arXiv:1305.7421 [hep-ph].

- [85] M. Nahrgang, J. Aichelin, P. B. Gossiaux, and K. Werner, “Influence of hadronic bound states above T_c on heavy-quark observables in Pb–Pb collisions at the CERN Large Hadron Collider,” *Phys.Rev.* **C89** no. 1, (2014) 014905, arXiv:1305.6544 [hep-ph].
- [86] S. Cao, G.-Y. Qin, and S. A. Bass, “Heavy-quark dynamics and hadronization in ultrarelativistic heavy-ion collisions: Collisional versus radiative energy loss,” *Phys. Rev.* **C88** (2013) 044907, arXiv:1308.0617 [nucl-th].

A The ALICE Collaboration

S. Acharya¹³⁹, F.T.-. Acosta²⁰, D. Adamová⁹³, J. Adolfsson⁸⁰, M.M. Aggarwal⁹⁸, G. Aglieri Rinella³⁴, M. Agnello³¹, N. Agrawal⁴⁸, Z. Ahammed¹³⁹, S.U. Ahn⁷⁶, S. Aiola¹⁴⁴, A. Akindinov⁶⁴, M. Al-Turany¹⁰⁴, S.N. Alam¹³⁹, D.S.D. Albuquerque¹²¹, D. Aleksandrov⁸⁷, B. Alessandro⁵⁸, R. Alfaro Molina⁷², Y. Ali¹⁵, A. Alici^{10, 53, 27}, A. Alkin², J. Alme²², T. Alt⁶⁹, L. Altenkamper²², I. Altsybeev¹¹¹, M.N. Anaam⁶, C. Andrei⁴⁷, D. Andreou³⁴, H.A. Andrews¹⁰⁸, A. Andronic^{142, 104}, M. Angeletti³⁴, V. Anguelov¹⁰², C. Anson¹⁶, T. Antičić¹⁰⁵, F. Antinori⁵⁶, P. Antonioli⁵³, R. Anwar¹²⁵, N. Apadula⁷⁹, L. Aphecetche¹¹³, H. Appelshäuser⁶⁹, S. Arcelli²⁷, R. Arnaldi⁵⁸, O.W. Arnold^{103, 116}, I.C. Arsene²¹, M. Arslanok¹⁰², A. Augustinus³⁴, R. Averbeck¹⁰⁴, M.D. Azmi¹⁷, A. Badalà⁵⁵, Y.W. Baek^{60, 40}, S. Bagnasco⁵⁸, R. Bailhache⁶⁹, R. Bala⁹⁹, A. Baldisseri¹³⁵, M. Ball⁴², R.C. Baral⁸⁵, A.M. Barbano²⁶, R. Barbera²⁸, F. Barile⁵², L. Barioglio²⁶, G.G. Barnaföldi¹⁴³, L.S. Barnby⁹², V. Barret¹³², P. Bartalini⁶, K. Barth³⁴, E. Bartsch⁶⁹, N. Bastid¹³², S. Basu¹⁴¹, G. Batigne¹¹³, B. Batyunya⁷⁵, P.C. Batzing²¹, J.L. Bazo Alba¹⁰⁹, I.G. Bearden⁸⁸, H. Beck¹⁰², C. Bedda⁶³, N.K. Behera⁶⁰, I. Belikov¹³⁴, F. Bellini³⁴, H. Bello Martinez⁴⁴, R. Bellwied¹²⁵, L.G.E. Beltran¹¹⁹, V. Belyaev⁹¹, G. Bencedi¹⁴³, S. Beole²⁶, A. Bercuci⁴⁷, Y. Berdnikov⁹⁶, D. Berenyi¹⁴³, R.A. Bertens¹²⁸, D. Berzano^{34, 58}, L. Betev³⁴, P.P. Bhaduri¹³⁹, A. Bhasin⁹⁹, I.R. Bhat⁹⁹, H. Bhatt⁴⁸, B. Bhattacharjee⁴¹, J. Bhom¹¹⁷, A. Bianchi²⁶, L. Bianchi¹²⁵, N. Bianchi⁵¹, J. Bielčik³⁷, J. Bielčiková⁹³, A. Bilandžić^{116, 103}, G. Biro¹⁴³, R. Biswas³, S. Biswas³, J.T. Blair¹¹⁸, D. Blau⁸⁷, C. Blume⁶⁹, G. Boca¹³⁷, F. Bock³⁴, A. Bogdanov⁹¹, L. Boldizsár¹⁴³, M. Bombara³⁸, G. Bonomi¹³⁸, M. Bonora³⁴, H. Borel¹³⁵, A. Borissov¹⁴², M. Borri¹²⁷, E. Botta²⁶, C. Bourjau⁸⁸, L. Bratrud⁶⁹, P. Braun-Munzinger¹⁰⁴, M. Bregant¹²⁰, T.A. Broker⁶⁹, M. Broz³⁷, E.J. Brucken⁴³, E. Bruna⁵⁸, G.E. Bruno^{34, 33}, D. Budnikov¹⁰⁶, H. Buesching⁶⁹, S. Bufalino³¹, P. Buhler¹¹², P. Buncic³⁴, O. Busch^{131, i}, Z. Buthelezi⁷³, J.B. Butt¹⁵, J.T. Buxton⁹⁵, J. Cabala¹¹⁵, D. Caffarri⁸⁹, H. Caines¹⁴⁴, A. Caliva¹⁰⁴, E. Calvo Villar¹⁰⁹, R.S. Camacho⁴⁴, P. Camerini²⁵, A.A. Capon¹¹², F. Carena³⁴, W. Carena³⁴, F. Carnesecchi^{27, 10}, J. Castillo Castellanos¹³⁵, A.J. Castro¹²⁸, E.A.R. Casula⁵⁴, C. Ceballos Sanchez⁸, S. Chandra¹³⁹, B. Chang¹²⁶, W. Chang⁶, S. Chapeland³⁴, M. Chartier¹²⁷, S. Chattopadhyay¹³⁹, S. Chattopadhyay¹⁰⁷, A. Chauvin^{103, 116}, C. Cheshkov¹³³, B. Cheynis¹³³, V. Chibante Barroso³⁴, D.D. Chinellato¹²¹, S. Cho⁶⁰, P. Chochula³⁴, T. Chowdhury¹³², P. Christakoglou⁸⁹, C.H. Christensen⁸⁸, P. Christiansen⁸⁰, T. Chujo¹³¹, S.U. Chung¹⁸, C. Cicalo⁵⁴, L. Cifarelli^{10, 27}, F. Cindolo⁵³, J. Cleymans¹²⁴, F. Colamaria⁵², D. Colella^{65, 52}, A. Collu⁷⁹, M. Colocci²⁷, M. Concas^{58, ii}, G. Conesa Balbastre⁷⁸, Z. Conesa del Valle⁶¹, J.G. Contreras³⁷, T.M. Cormier⁹⁴, Y. Corrales Morales⁵⁸, P. Cortese³², M.R. Cosentino¹²², F. Costa³⁴, S. Costanza¹³⁷, J. Crkovská⁶¹, P. Crochet¹³², E. Cuautle⁷⁰, L. Cunqueiro^{142, 94}, T. Dahms^{103, 116}, A. Dainese⁵⁶, S. Dani⁶⁶, M.C. Danisch¹⁰², A. Danu⁶⁸, D. Das¹⁰⁷, I. Das¹⁰⁷, S. Das³, A. Dash⁸⁵, S. Dash⁴⁸, S. De⁴⁹, A. De Caro³⁰, G. de Cataldo⁵², C. de Conti¹²⁰, J. de Cuveland³⁹, A. De Falco²⁴, D. De Gruttola^{10, 30}, N. De Marco⁵⁸, S. De Pasquale³⁰, R.D. De Souza¹²¹, H.F. Degenhardt¹²⁰, A. Deisting^{104, 102}, A. Deloff⁸⁴, S. Delsanto²⁶, C. Deplano⁸⁹, P. Dhankher⁴⁸, D. Di Bari³³, A. Di Mauro³⁴, B. Di Ruzza⁵⁶, R.A. Diaz⁸, T. Dietel¹²⁴, P. Dillenseger⁶⁹, Y. Ding⁶, R. Divià³⁴, Ø. Djuvsland²², A. Dobrin³⁴, D. Domenicis Gimenez¹²⁰, B. Dönigus⁶⁹, O. Dordic²¹, L.V.R. Doremalen⁶³, A.K. Dubey¹³⁹, A. Dubla¹⁰⁴, L. Ducroux¹³³, S. Dudi⁹⁸, A.K. Duggal⁹⁸, M. Dukhishyam⁸⁵, P. Dupieux¹³², R.J. Ehlers¹⁴⁴, D. Elia⁵², E. Endress¹⁰⁹, H. Engel⁷⁴, E. Eppe¹⁴⁴, B. Erasmus¹¹³, F. Erhardt⁹⁷, M.R. Ersdal²², B. Espagnon⁶¹, G. Eulisse³⁴, J. Eum¹⁸, D. Evans¹⁰⁸, S. Evdokimov⁹⁰, L. Fabbietti^{103, 116}, M. Faggin²⁹, J. Faivre⁷⁸, A. Fantoni⁵¹, M. Fasel⁹⁴, L. Feldkamp¹⁴², A. Feliciello⁵⁸, G. Feofilov¹¹¹, A. Fernández Téllez⁴⁴, A. Ferretti²⁶, A. Festanti³⁴, V.J.G. Feuillard¹⁰², J. Figiel¹¹⁷, M.A.S. Figueredo¹²⁰, S. Filchagin¹⁰⁶, D. Finogeev⁶², F.M. Fionda²², G. Fiorenza⁵², F. Flor¹²⁵, M. Floris³⁴, S. Foertsch⁷³, P. Foka¹⁰⁴, S. Fokin⁸⁷, E. Fragiaco⁵⁹, A. Francescon³⁴, A. Francisco¹¹³, U. Frankenfeld¹⁰⁴, G.G. Fronze²⁶, U. Fuchs³⁴, C. Furget⁷⁸, A. Furs⁶², M. Fusco Girard³⁰, J.J. Gaardhøje⁸⁸, M. Gagliardi²⁶, A.M. Gago¹⁰⁹, K. Gajdosova⁸⁸, M. Gallio²⁶, C.D. Galvan¹¹⁹, P. Ganoti⁸³, C. Garabatos¹⁰⁴, E. Garcia-Solis¹¹, K. Garg²⁸, C. Gargiulo³⁴, P. Gasik^{116, 103}, E.F. Gauger¹¹⁸, M.B. Gay Ducati⁷¹, M. Germain¹¹³, J. Ghosh¹⁰⁷, P. Ghosh¹³⁹, S.K. Ghosh³, P. Gianotti⁵¹, P. Giubellino^{104, 58}, P. Giubilato²⁹, P. Glässel¹⁰², D.M. Gómez Coral⁷², A. Gomez Ramirez⁷⁴, V. Gonzalez¹⁰⁴, P. González-Zamora⁴⁴, S. Gorbunov³⁹, L. Görlich¹¹⁷, S. Gotovac³⁵, V. Grabski⁷², L.K. Graczykowski¹⁴⁰, K.L. Graham¹⁰⁸, L. Greiner⁷⁹, A. Grelli⁶³, C. Grigoras³⁴, V. Grigoriev⁹¹, A. Grigoryan¹, S. Grigoryan⁷⁵, J.M. Gronefeld¹⁰⁴, F. Grosa³¹, J.F. Grosse-Oetringhaus³⁴, R. Grosso¹⁰⁴, R. Guernane⁷⁸, B. Guerzoni²⁷, M. Guittiere¹¹³, K. Gulbrandsen⁸⁸, T. Gunji¹³⁰, A. Gupta⁹⁹, R. Gupta⁹⁹, I.B. Guzman⁴⁴, R. Haake³⁴, M.K. Habib¹⁰⁴, C. Hadjidakis⁶¹, H. Hamagaki⁸¹, G. Hamar¹⁴³, M. Hamid⁶, J.C. Hamon¹³⁴, R. Hannigan¹¹⁸, M.R. Haque⁶³, A. Harlanderova¹⁰⁴, J.W. Harris¹⁴⁴, A. Harton¹¹, H. Hassan⁷⁸, D. Hatzifotiadou^{53, 10}, S. Hayashi¹³⁰, S.T. Heckel⁶⁹, E. Hellbär⁶⁹, H. Helstrup³⁶, A. Herghelegiu⁴⁷, E.G. Hernandez⁴⁴, G. Herrera Corral⁹, F. Herrmann¹⁴², K.F. Hetland³⁶, T.E. Hilden⁴³, H. Hillemanns³⁴, C. Hills¹²⁷, B. Hippolyte¹³⁴, B. Hohlweiger¹⁰³, D. Horak³⁷, S. Hornung¹⁰⁴, R. Hosokawa^{131, 78}, J. Hota⁶⁶, P. Hristov³⁴, C. Huang⁶¹,

C. Hughes¹²⁸, P. Huhn⁶⁹, T.J. Humanic⁹⁵, H. Hushnud¹⁰⁷, N. Hussain⁴¹, T. Hussain¹⁷, D. Hutter³⁹, D.S. Hwang¹⁹, J.P. Iddon¹²⁷, S.A. Iga Buitron⁷⁰, R. Ilkaev¹⁰⁶, M. Inaba¹³¹, M. Ippolitov⁸⁷, M.S. Islam¹⁰⁷, M. Ivanov¹⁰⁴, V. Ivanov⁹⁶, V. Izucheev⁹⁰, B. Jacak⁷⁹, N. Jacazio²⁷, P.M. Jacobs⁷⁹, M.B. Jadhav⁴⁸, S. Jadlovská¹¹⁵, J. Jadlovsky¹¹⁵, S. Jaelani⁶³, C. Jahnke^{120,116}, M.J. Jakubowska¹⁴⁰, M.A. Janik¹⁴⁰, C. Jena⁸⁵, M. Jercic⁹⁷, O. Jevons¹⁰⁸, R.T. Jimenez Bustamante¹⁰⁴, M. Jin¹²⁵, P.G. Jones¹⁰⁸, A. Jusko¹⁰⁸, P. Kalinak⁶⁵, A. Kalweit³⁴, J.H. Kang¹⁴⁵, V. Kaplin⁹¹, S. Kar⁶, A. Karasu Uysal⁷⁷, O. Karavichev⁶², T. Karavicheva⁶², P. Karczmarczyk³⁴, E. Karpechev⁶², U. Kebschull⁷⁴, R. Keidel⁴⁶, D.L.D. Keijdener⁶³, M. Keil³⁴, B. Ketzer⁴², Z. Khabanova⁸⁹, A.M. Khan⁶, S. Khan¹⁷, S.A. Khan¹³⁹, A. Khanzadeev⁹⁶, Y. Kharlov⁹⁰, A. Khatun¹⁷, A. Khuntia⁴⁹, M.M. Kielbowicz¹¹⁷, B. Kileng³⁶, B. Kim¹³¹, D. Kim¹⁴⁵, D.J. Kim¹²⁶, E.J. Kim¹³, H. Kim¹⁴⁵, J.S. Kim⁴⁰, J. Kim¹⁰², M. Kim^{102,60}, S. Kim¹⁹, T. Kim¹⁴⁵, T. Kim¹⁴⁵, S. Kirsch³⁹, I. Kisel³⁹, S. Kiselev⁶⁴, A. Kisiel¹⁴⁰, J.L. Klay⁵, C. Klein⁶⁹, J. Klein^{34,58}, C. Klein-Bösing¹⁴², S. Klewin¹⁰², A. Kluge³⁴, M.L. Knichel³⁴, A.G. Knospe¹²⁵, C. Kobdaj¹¹⁴, M. Kofarago¹⁴³, M.K. Köhler¹⁰², T. Kollegger¹⁰⁴, N. Kondratyeva⁹¹, E. Kondratyuk⁹⁰, A. Konevskikh⁶², P.J. Konopka³⁴, M. Konyushikhin¹⁴¹, O. Kovalenko⁸⁴, V. Kovalenko¹¹¹, M. Kowalski¹¹⁷, I. Králik⁶⁵, A. Kravčáková³⁸, L. Kreis¹⁰⁴, M. Krivda^{65,108}, F. Krizek⁹³, M. Krüger⁶⁹, E. Kryshen⁹⁶, M. Krzewicki³⁹, A.M. Kubera⁹⁵, V. Kučera^{60,93}, C. Kuhn¹³⁴, P.G. Kuijter⁸⁹, J. Kumar⁴⁸, L. Kumar⁹⁸, S. Kumar⁴⁸, S. Kundu⁸⁵, P. Kurashvili⁸⁴, A. Kurepin⁶², A.B. Kurepin⁶², A. Kuryakin¹⁰⁶, S. Kuschpil⁹³, J. Kvapil¹⁰⁸, M.J. Kweon⁶⁰, Y. Kwon¹⁴⁵, S.L. La Pointe³⁹, P. La Rocca²⁸, Y.S. Lai⁷⁹, I. Lakomov³⁴, R. Langoy¹²³, K. Lapidus¹⁴⁴, A. Lardeux²¹, P. Larionov⁵¹, E. Laudi³⁴, R. Lavicka³⁷, R. Lea²⁵, L. Leardini¹⁰², S. Lee¹⁴⁵, F. Lehas⁸⁹, S. Lehner¹¹², J. Lehrbach³⁹, R.C. Lemmon⁹², I. León Monzón¹¹⁹, P. Lévai¹⁴³, X. Li¹², X.L. Li⁶, J. Lien¹²³, R. Lietava¹⁰⁸, B. Lim¹⁸, S. Lindal²¹, V. Lindenstruth³⁹, S.W. Lindsay¹²⁷, C. Lippmann¹⁰⁴, M.A. Lisa⁹⁵, V. Litichevskiy⁴³, A. Liu⁷⁹, H.M. Ljunggren⁸⁰, W.J. Llope¹⁴¹, D.F. Lodato⁶³, V. Loginov⁹¹, C. Loizides^{94,79}, P. Loncar³⁵, X. Lopez¹³², E. López Torres⁸, A. Lowe¹⁴³, P. Luettig⁶⁹, J.R. Luhder¹⁴², M. Lunardon²⁹, G. Luparello⁵⁹, M. Lupi³⁴, A. Maevskaya⁶², M. Mager³⁴, S.M. Mahmood²¹, A. Maire¹³⁴, R.D. Majka¹⁴⁴, M. Malaev⁹⁶, Q.W. Malik²¹, L. Malinina^{75,iii}, D. Mal'Kevich⁶⁴, P. Malzacher¹⁰⁴, A. Mamonov¹⁰⁶, V. Manko⁸⁷, F. Manso¹³², V. Manzari⁵², Y. Mao⁶, M. Marchisone^{129,73,133}, J. Mareš⁶⁷, G.V. Margagliotti²⁵, A. Margotti⁵³, J. Margutti⁶³, A. Marín¹⁰⁴, C. Markert¹¹⁸, M. Marquard⁶⁹, N.A. Martin¹⁰⁴, P. Martinengo³⁴, J.L. Martinez¹²⁵, M.I. Martínez⁴⁴, G. Martínez García¹¹³, M. Martinez Pedreira³⁴, S. Masciocchi¹⁰⁴, M. Masera²⁶, A. Masoni⁵⁴, L. Massacrier⁶¹, E. Masson¹¹³, A. Mastroserio^{52,136}, A.M. Mathis^{116,103}, P.F.T. Matuoka¹²⁰, A. Matyja^{117,128}, C. Mayer¹¹⁷, M. Mazzilli³³, M.A. Mazzoni⁵⁷, F. Meddi²³, Y. Melikyan⁹¹, A. Menchaca-Rocha⁷², E. Meninno³⁰, J. Mercado Pérez¹⁰², M. Meres¹⁴, C.S. Meza¹⁰⁹, S. Mhlanga¹²⁴, Y. Miake¹³¹, L. Micheletti²⁶, M.M. Mieskolainen⁴³, D.L. Mihaylov¹⁰³, K. Mikhaylov^{64,75}, A. Mischke⁶³, A.N. Mishra⁷⁰, D. Miśkowiec¹⁰⁴, J. Mitra¹³⁹, C.M. Mitu⁶⁸, N. Mohammadi³⁴, A.P. Mohanty⁶³, B. Mohanty⁸⁵, M. Mohisin Khan^{17,iv}, D.A. Moreira De Godoy¹⁴², L.A.P. Moreno⁴⁴, S. Moretto²⁹, A. Morreale¹¹³, A. Morsch³⁴, T. Mrnjavac³⁴, V. Muccifora⁵¹, E. Mudnic³⁵, D. Mühlheim¹⁴², S. Muhuri¹³⁹, M. Mukherjee³, J.D. Mulligan¹⁴⁴, M.G. Munhoz¹²⁰, K. Mürning⁴², M.I.A. Muñoz⁷⁹, R.H. Munzer⁶⁹, H. Murakami¹³⁰, S. Murray⁷³, L. Musa³⁴, J. Musinsky⁶⁵, C.J. Myers¹²⁵, J.W. Myrcha¹⁴⁰, B. Naik⁴⁸, R. Nair⁸⁴, B.K. Nandi⁴⁸, R. Nania^{53,10}, E. Nappi⁵², A. Narayan⁴⁸, M.U. Naru¹⁵, A.F. Nassirpour⁸⁰, H. Natal da Luz¹²⁰, C. Nattrass¹²⁸, S.R. Navarro⁴⁴, K. Nayak⁸⁵, R. Nayak⁴⁸, T.K. Nayak¹³⁹, S. Nazarenko¹⁰⁶, R.A. Negrao De Oliveira^{69,34}, L. Nellen⁷⁰, S.V. Nesbo³⁶, G. Neskovic³⁹, F. Ng¹²⁵, M. Nicassio¹⁰⁴, J. Niedziela^{140,34}, B.S. Nielsen⁸⁸, S. Nikolaev⁸⁷, S. Nikulin⁸⁷, V. Nikulin⁹⁶, F. Noferini^{10,53}, P. Nomokonov⁷⁵, G. Nooren⁶³, J.C.C. Noris⁴⁴, J. Norman⁷⁸, A. Nyanin⁸⁷, J. Nystrand²², H. Oh¹⁴⁵, A. Ohlson¹⁰², J. Oleniacz¹⁴⁰, A.C. Oliveira Da Silva¹²⁰, M.H. Oliver¹⁴⁴, J. Onderwaater¹⁰⁴, C. Oppedisano⁵⁸, R. Orava⁴³, M. Oravec¹¹⁵, A. Ortiz Velasquez⁷⁰, A. Oskarsson⁸⁰, J. Otwinowski¹¹⁷, K. Oyama⁸¹, Y. Pachmayer¹⁰², V. Pacik⁸⁸, D. Pagano¹³⁸, G. Paic⁷⁰, P. Palni⁶, J. Pan¹⁴¹, A.K. Pandey⁴⁸, S. Panebianco¹³⁵, V. Papikyan¹, P. Pareek⁴⁹, J. Park⁶⁰, J.E. Parkkila¹²⁶, S. Parmar⁹⁸, A. Passfeld¹⁴², S.P. Pathak¹²⁵, R.N. Patra¹³⁹, B. Paul⁵⁸, H. Pei⁶, T. Peitzmann⁶³, X. Peng⁶, L.G. Pereira⁷¹, H. Pereira Da Costa¹³⁵, D. Peresunko⁸⁷, E. Perez Lezama⁶⁹, V. Peskov⁶⁹, Y. Pestov⁴, V. Petráček³⁷, M. Petrovici⁴⁷, C. Petta²⁸, R.P. Pezzi⁷¹, S. Piano⁵⁹, M. Pikna¹⁴, P. Pillot¹¹³, L.O.D.L. Pimentel⁸⁸, O. Pinazza^{53,34}, L. Pinsky¹²⁵, S. Pisano⁵¹, D.B. Piyarathna¹²⁵, M. Płoskoń⁷⁹, M. Planinic⁹⁷, F. Pliquett⁶⁹, J. Pluta¹⁴⁰, S. Pochybova¹⁴³, P.L.M. Podesta-Lerma¹¹⁹, M.G. Poghosyan⁹⁴, B. Polichtchouk⁹⁰, N. Poljak⁹⁷, W. Poonsawat¹¹⁴, A. Pop⁴⁷, H. Poppenberg¹⁴², S. Porteboeuf-Houssais¹³², V. Pozdniakov⁷⁵, S.K. Prasad³, R. Preghenella⁵³, F. Prino⁵⁸, C.A. Pruneau¹⁴¹, I. Pshenichnov⁶², M. Puccio²⁶, V. Punin¹⁰⁶, J. Putschke¹⁴¹, S. Raha³, S. Rajput⁹⁹, J. Rak¹²⁶, A. Rakotozafindrabe¹³⁵, L. Ramello³², F. Rami¹³⁴, R. Raniwala¹⁰⁰, S. Raniwala¹⁰⁰, S.S. Räsänen⁴³, B.T. Rascanu⁶⁹, V. Ratza⁴², I. Ravasenga³¹, K.F. Read^{128,94}, K. Redlich^{84,v}, A. Rehman²², P. Reichelt⁶⁹, F. Reidt³⁴, X. Ren⁶, R. Renfordt⁶⁹, A. Reshetin⁶², J.-P. Revol¹⁰, K. Reygers¹⁰², V. Riabov⁹⁶, T. Richert⁶³, M. Richter²¹, P. Riedler³⁴, W. Riegler³⁴, F. Riggi²⁸, C. Ristea⁶⁸, S.P. Rode⁴⁹,

M. Rodríguez Cahuantzi⁴⁴, K. Røed²¹, R. Rogalev⁹⁰, E. Rogochaya⁷⁵, D. Rohr³⁴, D. Röhrich²², P.S. Rokita¹⁴⁰, F. Ronchetti⁵¹, E.D. Rosas⁷⁰, K. Roslon¹⁴⁰, P. Rosnet¹³², A. Rossi²⁹, A. Rotondi¹³⁷, F. Roukoutakis⁸³, C. Roy¹³⁴, P. Roy¹⁰⁷, O.V. Rueda⁷⁰, R. Rui²⁵, B. Rumyantsev⁷⁵, A. Rustamov⁸⁶, E. Ryabinkin⁸⁷, Y. Ryabov⁹⁶, A. Rybicki¹¹⁷, S. Saarinen⁴³, S. Sadhu¹³⁹, S. Sadovsky⁹⁰, K. Šafařík³⁴, S.K. Saha¹³⁹, B. Sahoo⁴⁸, P. Sahoo⁴⁹, R. Sahoo⁴⁹, S. Sahoo⁶⁶, P.K. Sahu⁶⁶, J. Saini¹³⁹, S. Sakai¹³¹, M.A. Saleh¹⁴¹, S. Sambyal⁹⁹, V. Samsonov^{96,91}, A. Sandoval⁷², A. Sarkar⁷³, D. Sarkar¹³⁹, N. Sarkar¹³⁹, P. Sarma⁴¹, M.H.P. Sas⁶³, E. Scapparone⁵³, F. Scarlassara²⁹, B. Schaefer⁹⁴, H.S. Scheid⁶⁹, C. Schiaua⁴⁷, R. Schicker¹⁰², C. Schmidt¹⁰⁴, H.R. Schmidt¹⁰¹, M.O. Schmidt¹⁰², M. Schmidt¹⁰¹, N.V. Schmidt^{94,69}, J. Schukraft³⁴, Y. Schutz^{34,134}, K. Schwarz¹⁰⁴, K. Schweda¹⁰⁴, G. Scioli²⁷, E. Scomparin⁵⁸, M. Šefčík³⁸, J.E. Seger¹⁶, Y. Sekiguchi¹³⁰, D. Sekihata⁴⁵, I. Selyuzhenkov^{104,91}, S. Senyukov¹³⁴, E. Serradilla⁷², P. Sett⁴⁸, A. Sevcenco⁶⁸, A. Shabanov⁶², A. Shabetai¹¹³, R. Shahoyan³⁴, W. Shaikh¹⁰⁷, A. Shangaraev⁹⁰, A. Sharma⁹⁸, A. Sharma⁹⁹, M. Sharma⁹⁹, N. Sharma⁹⁸, A.I. Sheikh¹³⁹, K. Shigaki⁴⁵, M. Shimomura⁸², S. Shirinkin⁶⁴, Q. Shou^{6,110}, K. Shtejer²⁶, Y. Sibiriak⁸⁷, S. Siddhanta⁵⁴, K.M. Sielewicz³⁴, T. Siemiarczuk⁸⁴, D. Silvermyr⁸⁰, G. Simatovic⁸⁹, G. Simonetti^{34,103}, R. Singaraju¹³⁹, R. Singh⁸⁵, R. Singh⁹⁹, V. Singhal¹³⁹, T. Sinha¹⁰⁷, B. Sitar¹⁴, M. Sitta³², T.B. Skaali²¹, M. Slupecki¹²⁶, N. Smirnov¹⁴⁴, R.J.M. Snellings⁶³, T.W. Snellman¹²⁶, J. Song¹⁸, F. Soramel²⁹, S. Sorensen¹²⁸, F. Sozzi¹⁰⁴, I. Sputowska¹¹⁷, J. Stachel¹⁰², I. Stan⁶⁸, P. Stankus⁹⁴, E. Stenlund⁸⁰, D. Stocco¹¹³, M.M. Stortvedt³⁶, P. Strmen¹⁴, A.A.P. Suaide¹²⁰, T. Sugitate⁴⁵, C. Suire⁶¹, M. Suleymanov¹⁵, M. Suljic^{34,25}, R. Sultanov⁶⁴, M. Šumbera⁹³, S. Sumowidagdo⁵⁰, K. Suzuki¹¹², S. Swain⁶⁶, A. Szabo¹⁴, I. Szarka¹⁴, U. Tabassam¹⁵, J. Takahashi¹²¹, G.J. Tambave²², N. Tanaka¹³¹, M. Tarhini¹¹³, M. Tariq¹⁷, M.G. Tarzila⁴⁷, A. Tauro³⁴, G. Tejada Muñoz⁴⁴, A. Telesca³⁴, C. Terrevoli²⁹, B. Teyssier¹³³, D. Thakur⁴⁹, S. Thakur¹³⁹, D. Thomas¹¹⁸, F. Thoresen⁸⁸, R. Tieulent¹³³, A. Tikhonov⁶², A.R. Timmins¹²⁵, A. Toia⁶⁹, N. Topilskaya⁶², M. Toppi⁵¹, S.R. Torres¹¹⁹, S. Tripathy⁴⁹, S. Trogolo²⁶, G. Trombetta³³, L. Tropp³⁸, V. Trubnikov², W.H. Trzaska¹²⁶, T.P. Trzcinski¹⁴⁰, B.A. Trzeciak⁶³, T. Tsuji¹³⁰, A. Tumkin¹⁰⁶, R. Turrisi⁵⁶, T.S. Tveter²¹, K. Ullaland²², E.N. Umaka¹²⁵, A. Uras¹³³, G.L. Usai²⁴, A. Utrobicic⁹⁷, M. Vala¹¹⁵, J.W. Van Hoorne³⁴, M. van Leeuwen⁶³, P. Vande Vyvre³⁴, D. Varga¹⁴³, A. Vargas⁴⁴, M. Vargyas¹²⁶, R. Varma⁴⁸, M. Vasileiou⁸³, A. Vasiliev⁸⁷, A. Vauthier⁷⁸, O. Vázquez Doce^{103,116}, V. Vechernin¹¹¹, A.M. Veen⁶³, E. Vercellin²⁶, S. Vergara Limón⁴⁴, L. Vermunt⁶³, R. Vernet⁷, R. Vértesi¹⁴³, L. Vickovic³⁵, J. Viinikainen¹²⁶, Z. Vilakazi¹²⁹, O. Villalobos Baillie¹⁰⁸, A. Villatoro Tello⁴⁴, A. Vinogradov⁸⁷, T. Virgili³⁰, V. Vislavicius^{88,80}, A. Vodopyanov⁷⁵, M.A. Völk¹⁰¹, K. Voloshin⁶⁴, S.A. Voloshin¹⁴¹, G. Volpe³³, B. von Haller³⁴, I. Vorobyev^{116,103}, D. Voscek¹¹⁵, D. Vranic^{104,34}, J. Vrláková³⁸, B. Wagner²², H. Wang⁶³, M. Wang⁶, Y. Watanabe¹³¹, M. Weber¹¹², S.G. Weber¹⁰⁴, A. Wegrzynek³⁴, D.F. Weiser¹⁰², S.C. Wenzel³⁴, J.P. Wessels¹⁴², U. Westerhoff¹⁴², A.M. Whitehead¹²⁴, J. Wiechula⁶⁹, J. Wikne²¹, G. Wilk⁸⁴, J. Wilkinson⁵³, G.A. Willems^{142,34}, M.C.S. Williams⁵³, E. Willsher¹⁰⁸, B. Windelband¹⁰², W.E. Witt¹²⁸, R. Xu⁶, S. Yalcin⁷⁷, K. Yamakawa⁴⁵, S. Yano⁴⁵, Z. Yin⁶, H. Yokoyama^{78,131}, I.-K. Yoo¹⁸, J.H. Yoon⁶⁰, V. Yurchenko², V. Zaccolo⁵⁸, A. Zaman¹⁵, C. Zampolli³⁴, H.J.C. Zanolli¹²⁰, N. Zardoshti¹⁰⁸, A. Zarochentsev¹¹¹, P. Závada⁶⁷, N. Zaviyalov¹⁰⁶, H. Zbroszczyk¹⁴⁰, M. Zhalov⁹⁶, X. Zhang⁶, Y. Zhang⁶, Z. Zhang^{6,132}, C. Zhao²¹, V. Zhrebchevskii¹¹¹, N. Zhigareva⁶⁴, D. Zhou⁶, Y. Zhou⁸⁸, Z. Zhou²², H. Zhu⁶, J. Zhu⁶, Y. Zhu⁶, A. Zichichi^{27,10}, M.B. Zimmermann³⁴, G. Zinovjev², J. Zmeskal¹¹², S. Zou⁶,

Affiliation notes

ⁱ Deceased

ⁱⁱ Dipartimento DET del Politecnico di Torino, Turin, Italy

ⁱⁱⁱ M.V. Lomonosov Moscow State University, D.V. Skobeltsyn Institute of Nuclear Physics, Moscow, Russia

^{iv} Department of Applied Physics, Aligarh Muslim University, Aligarh, India

^v Institute of Theoretical Physics, University of Wrocław, Poland

Collaboration Institutes

¹ A.I. Alikhanyan National Science Laboratory (Yerevan Physics Institute) Foundation, Yerevan, Armenia

² Bogolyubov Institute for Theoretical Physics, National Academy of Sciences of Ukraine, Kiev, Ukraine

³ Bose Institute, Department of Physics and Centre for Astroparticle Physics and Space Science (CAPSS), Kolkata, India

⁴ Budker Institute for Nuclear Physics, Novosibirsk, Russia

⁵ California Polytechnic State University, San Luis Obispo, California, United States

⁶ Central China Normal University, Wuhan, China

⁷ Centre de Calcul de l'IN2P3, Villeurbanne, Lyon, France

- ⁸ Centro de Aplicaciones Tecnológicas y Desarrollo Nuclear (CEADEN), Havana, Cuba
- ⁹ Centro de Investigación y de Estudios Avanzados (CINVESTAV), Mexico City and Mérida, Mexico
- ¹⁰ Centro Fermi - Museo Storico della Fisica e Centro Studi e Ricerche “Enrico Fermi”, Rome, Italy
- ¹¹ Chicago State University, Chicago, Illinois, United States
- ¹² China Institute of Atomic Energy, Beijing, China
- ¹³ Chonbuk National University, Jeonju, Republic of Korea
- ¹⁴ Comenius University Bratislava, Faculty of Mathematics, Physics and Informatics, Bratislava, Slovakia
- ¹⁵ COMSATS Institute of Information Technology (CIIT), Islamabad, Pakistan
- ¹⁶ Creighton University, Omaha, Nebraska, United States
- ¹⁷ Department of Physics, Aligarh Muslim University, Aligarh, India
- ¹⁸ Department of Physics, Pusan National University, Pusan, Republic of Korea
- ¹⁹ Department of Physics, Sejong University, Seoul, Republic of Korea
- ²⁰ Department of Physics, University of California, Berkeley, California, United States
- ²¹ Department of Physics, University of Oslo, Oslo, Norway
- ²² Department of Physics and Technology, University of Bergen, Bergen, Norway
- ²³ Dipartimento di Fisica dell’Università ‘La Sapienza’ and Sezione INFN, Rome, Italy
- ²⁴ Dipartimento di Fisica dell’Università and Sezione INFN, Cagliari, Italy
- ²⁵ Dipartimento di Fisica dell’Università and Sezione INFN, Trieste, Italy
- ²⁶ Dipartimento di Fisica dell’Università and Sezione INFN, Turin, Italy
- ²⁷ Dipartimento di Fisica e Astronomia dell’Università and Sezione INFN, Bologna, Italy
- ²⁸ Dipartimento di Fisica e Astronomia dell’Università and Sezione INFN, Catania, Italy
- ²⁹ Dipartimento di Fisica e Astronomia dell’Università and Sezione INFN, Padova, Italy
- ³⁰ Dipartimento di Fisica ‘E.R. Caianiello’ dell’Università and Gruppo Collegato INFN, Salerno, Italy
- ³¹ Dipartimento DISAT del Politecnico and Sezione INFN, Turin, Italy
- ³² Dipartimento di Scienze e Innovazione Tecnologica dell’Università del Piemonte Orientale and INFN Sezione di Torino, Alessandria, Italy
- ³³ Dipartimento Interateneo di Fisica ‘M. Merlin’ and Sezione INFN, Bari, Italy
- ³⁴ European Organization for Nuclear Research (CERN), Geneva, Switzerland
- ³⁵ Faculty of Electrical Engineering, Mechanical Engineering and Naval Architecture, University of Split, Split, Croatia
- ³⁶ Faculty of Engineering and Science, Western Norway University of Applied Sciences, Bergen, Norway
- ³⁷ Faculty of Nuclear Sciences and Physical Engineering, Czech Technical University in Prague, Prague, Czech Republic
- ³⁸ Faculty of Science, P.J. Šafárik University, Košice, Slovakia
- ³⁹ Frankfurt Institute for Advanced Studies, Johann Wolfgang Goethe-Universität Frankfurt, Frankfurt, Germany
- ⁴⁰ Gangneung-Wonju National University, Gangneung, Republic of Korea
- ⁴¹ Gauhati University, Department of Physics, Guwahati, India
- ⁴² Helmholtz-Institut für Strahlen- und Kernphysik, Rheinische Friedrich-Wilhelms-Universität Bonn, Bonn, Germany
- ⁴³ Helsinki Institute of Physics (HIP), Helsinki, Finland
- ⁴⁴ High Energy Physics Group, Universidad Autónoma de Puebla, Puebla, Mexico
- ⁴⁵ Hiroshima University, Hiroshima, Japan
- ⁴⁶ Hochschule Worms, Zentrum für Technologietransfer und Telekommunikation (ZTT), Worms, Germany
- ⁴⁷ Horia Hulubei National Institute of Physics and Nuclear Engineering, Bucharest, Romania
- ⁴⁸ Indian Institute of Technology Bombay (IIT), Mumbai, India
- ⁴⁹ Indian Institute of Technology Indore, Indore, India
- ⁵⁰ Indonesian Institute of Sciences, Jakarta, Indonesia
- ⁵¹ INFN, Laboratori Nazionali di Frascati, Frascati, Italy
- ⁵² INFN, Sezione di Bari, Bari, Italy
- ⁵³ INFN, Sezione di Bologna, Bologna, Italy
- ⁵⁴ INFN, Sezione di Cagliari, Cagliari, Italy
- ⁵⁵ INFN, Sezione di Catania, Catania, Italy
- ⁵⁶ INFN, Sezione di Padova, Padova, Italy
- ⁵⁷ INFN, Sezione di Roma, Rome, Italy
- ⁵⁸ INFN, Sezione di Torino, Turin, Italy

- 59 INFN, Sezione di Trieste, Trieste, Italy
- 60 Inha University, Incheon, Republic of Korea
- 61 Institut de Physique Nucléaire d'Orsay (IPNO), Institut National de Physique Nucléaire et de Physique des Particules (IN2P3/CNRS), Université de Paris-Sud, Université Paris-Saclay, Orsay, France
- 62 Institute for Nuclear Research, Academy of Sciences, Moscow, Russia
- 63 Institute for Subatomic Physics, Utrecht University/Nikhef, Utrecht, Netherlands
- 64 Institute for Theoretical and Experimental Physics, Moscow, Russia
- 65 Institute of Experimental Physics, Slovak Academy of Sciences, Košice, Slovakia
- 66 Institute of Physics, Homi Bhabha National Institute, Bhubaneswar, India
- 67 Institute of Physics of the Czech Academy of Sciences, Prague, Czech Republic
- 68 Institute of Space Science (ISS), Bucharest, Romania
- 69 Institut für Kernphysik, Johann Wolfgang Goethe-Universität Frankfurt, Frankfurt, Germany
- 70 Instituto de Ciencias Nucleares, Universidad Nacional Autónoma de México, Mexico City, Mexico
- 71 Instituto de Física, Universidade Federal do Rio Grande do Sul (UFRGS), Porto Alegre, Brazil
- 72 Instituto de Física, Universidad Nacional Autónoma de México, Mexico City, Mexico
- 73 iThemba LABS, National Research Foundation, Somerset West, South Africa
- 74 Johann-Wolfgang-Goethe Universität Frankfurt Institut für Informatik, Fachbereich Informatik und Mathematik, Frankfurt, Germany
- 75 Joint Institute for Nuclear Research (JINR), Dubna, Russia
- 76 Korea Institute of Science and Technology Information, Daejeon, Republic of Korea
- 77 KTO Karatay University, Konya, Turkey
- 78 Laboratoire de Physique Subatomique et de Cosmologie, Université Grenoble-Alpes, CNRS-IN2P3, Grenoble, France
- 79 Lawrence Berkeley National Laboratory, Berkeley, California, United States
- 80 Lund University Department of Physics, Division of Particle Physics, Lund, Sweden
- 81 Nagasaki Institute of Applied Science, Nagasaki, Japan
- 82 Nara Women's University (NWU), Nara, Japan
- 83 National and Kapodistrian University of Athens, School of Science, Department of Physics, Athens, Greece
- 84 National Centre for Nuclear Research, Warsaw, Poland
- 85 National Institute of Science Education and Research, Homi Bhabha National Institute, Jatni, India
- 86 National Nuclear Research Center, Baku, Azerbaijan
- 87 National Research Centre Kurchatov Institute, Moscow, Russia
- 88 Niels Bohr Institute, University of Copenhagen, Copenhagen, Denmark
- 89 Nikhef, National institute for subatomic physics, Amsterdam, Netherlands
- 90 NRC Kurchatov Institute IHEP, Protvino, Russia
- 91 NRNU Moscow Engineering Physics Institute, Moscow, Russia
- 92 Nuclear Physics Group, STFC Daresbury Laboratory, Daresbury, United Kingdom
- 93 Nuclear Physics Institute of the Czech Academy of Sciences, Řež u Prahy, Czech Republic
- 94 Oak Ridge National Laboratory, Oak Ridge, Tennessee, United States
- 95 Ohio State University, Columbus, Ohio, United States
- 96 Petersburg Nuclear Physics Institute, Gatchina, Russia
- 97 Physics department, Faculty of science, University of Zagreb, Zagreb, Croatia
- 98 Physics Department, Panjab University, Chandigarh, India
- 99 Physics Department, University of Jammu, Jammu, India
- 100 Physics Department, University of Rajasthan, Jaipur, India
- 101 Physikalisches Institut, Eberhard-Karls-Universität Tübingen, Tübingen, Germany
- 102 Physikalisches Institut, Ruprecht-Karls-Universität Heidelberg, Heidelberg, Germany
- 103 Physik Department, Technische Universität München, Munich, Germany
- 104 Research Division and ExtreMe Matter Institute EMMI, GSI Helmholtzzentrum für Schwerionenforschung GmbH, Darmstadt, Germany
- 105 Rudjer Bošković Institute, Zagreb, Croatia
- 106 Russian Federal Nuclear Center (VNIIEF), Sarov, Russia
- 107 Saha Institute of Nuclear Physics, Homi Bhabha National Institute, Kolkata, India
- 108 School of Physics and Astronomy, University of Birmingham, Birmingham, United Kingdom
- 109 Sección Física, Departamento de Ciencias, Pontificia Universidad Católica del Perú, Lima, Peru

- 110 Shanghai Institute of Applied Physics, Shanghai, China
- 111 St. Petersburg State University, St. Petersburg, Russia
- 112 Stefan Meyer Institut für Subatomare Physik (SMI), Vienna, Austria
- 113 SUBATECH, IMT Atlantique, Université de Nantes, CNRS-IN2P3, Nantes, France
- 114 Suranaree University of Technology, Nakhon Ratchasima, Thailand
- 115 Technical University of Košice, Košice, Slovakia
- 116 Technische Universität München, Excellence Cluster 'Universe', Munich, Germany
- 117 The Henryk Niewodniczanski Institute of Nuclear Physics, Polish Academy of Sciences, Cracow, Poland
- 118 The University of Texas at Austin, Austin, Texas, United States
- 119 Universidad Autónoma de Sinaloa, Culiacán, Mexico
- 120 Universidade de São Paulo (USP), São Paulo, Brazil
- 121 Universidade Estadual de Campinas (UNICAMP), Campinas, Brazil
- 122 Universidade Federal do ABC, Santo Andre, Brazil
- 123 University College of Southeast Norway, Tonsberg, Norway
- 124 University of Cape Town, Cape Town, South Africa
- 125 University of Houston, Houston, Texas, United States
- 126 University of Jyväskylä, Jyväskylä, Finland
- 127 University of Liverpool, Liverpool, United Kingdom
- 128 University of Tennessee, Knoxville, Tennessee, United States
- 129 University of the Witwatersrand, Johannesburg, South Africa
- 130 University of Tokyo, Tokyo, Japan
- 131 University of Tsukuba, Tsukuba, Japan
- 132 Université Clermont Auvergne, CNRS/IN2P3, LPC, Clermont-Ferrand, France
- 133 Université de Lyon, Université Lyon 1, CNRS/IN2P3, IPN-Lyon, Villeurbanne, Lyon, France
- 134 Université de Strasbourg, CNRS, IPHC UMR 7178, F-67000 Strasbourg, France, Strasbourg, France
- 135 Université Paris-Saclay Centre d'Études de Saclay (CEA), IRFU, Department de Physique Nucléaire (DPhN), Saclay, France
- 136 Università degli Studi di Foggia, Foggia, Italy
- 137 Università degli Studi di Pavia, Pavia, Italy
- 138 Università di Brescia, Brescia, Italy
- 139 Variable Energy Cyclotron Centre, Homi Bhabha National Institute, Kolkata, India
- 140 Warsaw University of Technology, Warsaw, Poland
- 141 Wayne State University, Detroit, Michigan, United States
- 142 Westfälische Wilhelms-Universität Münster, Institut für Kernphysik, Münster, Germany
- 143 Wigner Research Centre for Physics, Hungarian Academy of Sciences, Budapest, Hungary
- 144 Yale University, New Haven, Connecticut, United States
- 145 Yonsei University, Seoul, Republic of Korea